ABSTRACT

ROGERS, BRYAN. Caspase-8 and FLIP Form a Dimer After Urea-Induced Unfolding. (Under the direction of Clay A. Clark).

Caspases initiate the cellular suicide pathway of apoptosis to delete damaged or unnecessary cells in organism development, immune system maintenance, and tissue homeostasis. The initiator procaspase-8 controls the fate of the cell by activating both proliferation and apoptotic pathways. In the well characterized apoptotic role of caspase-8, an extrinsic signal leads to the dimerization of two latent procaspase-8 monomers which self-activate upon induced proximity dimerization and activate caspase-3 by cleavage. In the less understood role of cell survival, procaspase-8 can heterodimerize with FLIP [FLICE (FADD-like interleukin 1 β converting enzyme) -inhibitory protein]. FLIP is homologous to procaspase-8 but lacks critical residues necessary for catalytic activity. There is evidence that procaspase-8 monomers may prefer heterodimerizering with FLIP over homodimerizing with another procaspase-8 monomer. The survival function of FLIP is therefore owed to its propensity to bind procaspase-8 monomers as a dominant negative inhibitor of the apoptotic pathway. Our study is a biophysical comparison of procaspase-8 and FLIP. We determined that procaspase-8 folds slowly by a two state mechanism and FLIP folds nearly 1000 s faster by a three-state mechanism. We also determined that by populating an intermediate of the FLIP folding pathway, we can achieve a propensity for heterodimerization and subsequent cleavage of intersubunit linker of FLIP.

Caspase-8 and FLIP Form a Dimer After Urea-Induced Unfolding

by
Bryan Rogers

A thesis submitted to the Graduate Faculty of
North Carolina State University
in partial fulfillment of the
requirements for the degree of
Master of Science

Biochemistry

Raleigh, North Carolina

2014

APPROVED BY:

_____	_____
Clay A. Clark Committee Chair	Robert Rose
_____	
Earl Maxwell	

DEDICATION

I dedicate this work to my wife Danielle and my family.

BIOGRAPHY

Bryan was born in New York and moved to Texas, Louisiana, Georgia, and North Carolina while growing up. After high school, he served as an ETN in the United States Navy before attending NCSU where he earned a Bachelor's degree in Biochemistry.

ACKNOWLEDGMENTS

Thank you Dr. Sarah MacKenzie

for everything you've taught me.

Thank you Dr. Clay Clark for the mentorship over beer

and Claymates for keeping things sincere.

TABLE OF CONTENTS

LIST OF TABLES

Chapter I

LIST OF FIGURES

CHAPTER I

Introduction

A. On the role of cell death in general organism health

Programmed cell death is fundamental to the development, regulation, and health of tissue homeostasis. Old, unnecessary, or damaged cells are culled using apoptosis and are replaced by new cells. Alteration of this complex pathway has far reaching consequences in pathology. If apoptosis occurs to cells heedlessly fails to occur entirely a wide range of diseases can occur (Table 1). As apoptosis is such a binary decision in the fate of the cell, determining how it can be initiated or thwarted is critical for developing therapies where dysregulation occurs. Caspases are the family of proteins that decide if and when apoptosis occurs and also have a multitude of non-apoptotic functions ranging from T-cell activation and cellular proliferation in caspase-8 alone.

Table 1			
Diseases caused by alterations in apoptosis			
Cancer	**Neurological disorders**	**Cardiovascular disorders**	**Autoimmune diseases**
Breast	Alzheimer	Ischemia	Systemic Lupus erythematosis
Lung	Parkinson	Heart Failure	Autoimmune lymphoproliferative syndrome
Kidney	Huntington	Infectious diseases	Rheumatoid arthritis
Ovary and uterus	Amytrophic Lateral Sclerosis	Bacterial	Thyroiditis
CNS	Stroke	Viral	
Gastro-enteric			

B. Caspase-8 structure

Caspase-8 is a cysteine-aspartate protease that exists in cells in its latent monomeric form as an initiator of apoptosis. The general caspase mechanism involves cleaving a substrate peptide after an aspartate residue using its active site cysteine to attack the peptide bond. This mechanism is a common feature among all caspases and thus caspases as a family have little substrate specificity between them. Substrate preference relies on the upstream and downstream residues of the aspartate residue being cleaved. For example, the caspase-3 substrate preference is D**E**VD and caspase-8 preferentially cleaves I**E**TD. Zymogen procaspase-8 is defined by a large and small subunit linked together by a flexible intersubunit linker adopting the typical caspase fold, that is, a six stranded beta sheet containing five parallel and one antiparallel beta strands surrounded by five alpha helices linked together by four loops. The active site is formed partially by loops 1 and 3 which are in a closed formation until rearrangement occurs upon homodimerization or heterodimerization and intersubunit linker cleavage.

B.1. FLIP Structure

FLIP is a monomeric homologue of procaspase-8 absent the catalytic residues thereby precluding FLIP from proteolytic activity. FLIP heterodimerizes with procaspase-8 activating it and changing its substrate repertoire allowing procaspase-8 to participate in distinct non-apoptotic pathways. There are three isoforms of FLIP that have been characterized: c-FLIP-long ($FLIP_{(L)}$), c-FLIP-short ($FLIP_{(S)}$), and c-$FLIP_{(R)}$. $FLIP_{(S)}$ is an isoform of FLIP that contains the prodomain and ten residues of the large subunit. FLIP(s) has been shown to completely inhibit caspase-8 activity upon heterodimerization acting as a dominant negative.

$FLIP_{(L)}$ is the form that activates caspase-8 and gives it unique substrate capabilities and will be referred to as simply FLIP for the remainder of this paper.

Importantly, caspase-8 and FLIP heterodimerize to form eight hydrogen bonds at the dimer interface whereas the caspase-8 homodimer only contains four [1]. Additionally, Arg 337 of FLIP's alpha helix 3 forms a hydrogen bond with Gln 450 of caspase-8. Having an additional interaction with FLIP's alpha helix 3 tethers the two molecules together tighter than the caspase-8 homodimer because its interface only has contacts between alpha helix 5 and beta sheet 6. This is confirmed as caspase-8 prefers to dimerize with FLIP rather than another caspase-8 monomer [2, 3]. Recently, an attempt at strengthening the caspase-8 dimer interface was made by optimizing the hydrophobic residues involved. This was done by removing the bulky residues thought to be negative design elements [4]. The results showed higher dimerization propensity and activity *in vitro* but no gain of apoptotic activity was seen *in vivo*. It is possible that the developed mutant caspase-8 proteins dimerized with FLIP with an even higher propensity. Caspase-8 activation or inactivation determines the fate of mammalian cells.

C. Caspase-dependent apoptosis

Apoptosis generally occurs through an intrinsic and extrinsic pathway (Figure 1). The extrinsic pathway is dependent upon the formation of the death inducing signaling complex (DISC) at the membrane bound receptor TNFR or FasR. An extracellular signal will cause a cascade of events culminating at the programmed disassembly of the cell. The intrinsic pathway occurs upon intracellular stress and employs the mitochondria to assist in the

activation of apoptosis. Both pathways converge upon on the cleavage and subsequent activation of caspase-3. Once this occurs little can be done to inhibit apoptosis.

C.1. Caspase family

The caspase family of proteins is divided into two groups based on their role in apoptosis: initiators and executioners (Figure 2). Initiator caspases initiate the caspase cascade and are normally kept a few steps away from being fully active. Zymogens of the initiator caspases (caspases-2, 8, and 9) are monomeric and require dimerization before they can initiate executioner caspases. Dimerization is a highly regulated process and helps to keep apoptosis from occurring accidentally. Although not required for activity, cleavage of the intersubunit linker after dimerization leads to a more stable enzyme. Self-cleavage can occur and other initiator caspases can cleave the intersubunit of caspase-8 as well. Executioner caspases (caspases-3, 6, and 7) exist in cells as an inactive dimer and are a single step away from full activation. Once an initiator has been activated by dimerization, it cleaves the intersubunit linker of an executioner caspase in order to carry out the cascade. Caspase-8 and caspase-9 both cleave caspase-3 in the extrinsic and intrinsic apoptotic pathway respectively.

C.2. Extrinsic apoptosis

A death ligand, such as TNF-α, forms a homotrimer made up of 26 kDa monomers. The TNF-α trimer will then bind to its death receptor TNFR causing oligomerization of the receptors which results in the recruitment of adapter proteins and activation of signaling events [5]. TNFR contains a death domain (DD) for recruiting proteins which also contain a DD such as the Fas-associated death domain (FADD) protein which also contains a death

effector domain (DED) [6]. The DED portion of FADD allows for it to recruit procaspase-8 through its shared DED to form the DISC (Figure 2). Procaspase-8 exists in cells in its latent, inactive zymogen form composed of a large and small subunit connected by an intersubunit linker. Once dimerized, caspase-8 will auto-process itself to cleave the catalytic domain from the protease domain thus releasing an active enzyme from the DISC [7]. The dimerized caspase-8 will also cleave off its own prodomain leaving the catalytic domain and the DED free in the cytosol. The activated caspase-8 will then cleave procaspase-3 to carry out execution of apoptosis [8]. There is growing evidence that the DEDs can also have a profound effect on the activation of apoptosis. It has been shown that the DEDs of caspase-8 can cause enhancement of apoptosis [9]. More recently, the DEDs aggregate with microtubules to induce apoptosis independent of caspase-8 presence. Paclitaxel causes cell death by induction of caspase-8 through this DED microtubule association suggesting that microtubules can serve as a scaffold for caspase-8 activation [10].

The regulation of caspase-8 in extrinsic apoptosis relies on preventing the formation of caspase-8 and inhibiting the activity of caspase-3 by FLIP and XIAP respectively. Caspase-8 can be tagged for ubiquitination on its p10 catalytic domain by the DISC containing molecule TRAF2 which interacts with the E3-ubiquitin ligase Cullin3 [11]. This allows for a shut off timer of caspase-8 once the catalytic domain is released in the cytosol.

In order for caspase-8 to dimerize, there must be a significantly larger pool of procaspase-8 monomers than FLIP monomers to outcompete FLIP [12] as caspase-8 monomers have a higher affinity for FLIP monomer than other caspase-8 monomers [3]. During caspase-dependent apoptosis, FLIP is down regulated by the inactivation of NFκB

[13]. It has recently been found through a high-throughput genome sequencing study that somatic mutations caspase-8 greatly diminishes apoptosis and increases NFκB activation when glycine 325 is mutated to a cysteine which causes an increase in epithelial tumor types [14].

C.3. Intrinsic apoptosis

Intrinsic apoptosis occurs as a result of intracellular stress such as irreparable DNA damage, chemotherapeutic agents, cytokines, and reactive oxygen species. This process begins with caspase-8 cleaving the pro-apoptotic protein Bid into truncated Bid (t-Bid) [15]. T-Bid then translocates into the mitochondria causing a change in the membrane potential allowing for the formation of small pores on the exterior of the mitochondria. Pro-apoptotic proteins are released from the pores such as Cytochrome c, SMAC, and DIABLO. SMAC and DIABLO are proteins that inhibit caspase inhibitors such as XIAP. Cytochrome C will form a large wheel-like complex with APAF-1. Caspase-9 will be recruited to this complex allowing for its dimerization and activation. Once activated, caspase-9 cleaves caspase-3 to carry out apoptosis. Intrinsic apoptosis is negatively regulated by the PI3K/Akt pathway where growth factors cause the phosphorylation of the proapoptotic protein BAD, thwarting apoptosis and allowing for cell survival [16]. XIAP is also a negative regulator of apoptosis and directly inhibits caspase-3 by placing an alpha-helix into its active site [17].

D. The non-apoptotic function of caspase-8

TNF-α is the ligand which is the external signals that serves as the origin death stimulus. Under normal cellular conditions, TNF-α signals for survival and cellular proliferation by the action of caspase-8. While a dimer of caspase-8 causes apoptosis, a

heterodimer of caspase-8 and FLIP causes proliferation. FLIP is a homologous protein to caspase-8 without the critical residues necessary for enzymatic activity. Originally thought of as simply an inhibitor of apoptosis, FLIP actually yields an active enzyme with a different substrate repertoire than that of the dimer [2]. The heterodimer couldn't have a more opposing effect on the cell than the homodimer of caspase-8: not only does it cause cell survival but it causes cellular proliferation.

D.1. TNFR1 promotes cell death and proliferation

Aside from signaling for cell death, TNFR1 also has functions of transducing a survival signal by promoting cell proliferation through the activation of NFκB. NFκB is activated in response to inflammatory stimuli such as IL1β. The pathway ends with the activation of the IKK complex, which is composed of IKKα, β, and γ. The target of the IKK complex is the NFκB inhibitor, IκB, which is phosphorylated and subsequently ubiquitinated for proteosomal degradation. This allows for the translocation of the transcription factor NFκB into the nucleus resulting in gene activation [18]. NFκB inhibits apoptosis by expressing FLIP and causes proliferation by activating cell cycle progression proteins such as CDK4.

D.2. Necroptosis and caspase-8

The function of the heterodimer is an absolute requirement for normal tissue development as mice without caspase-8 die in embryonic day 8-10 [19]. The non-apoptotic role of caspase-8 is steeped in its involvement of immune function as T-cell activation and development require both caspase-8 and FLIP [20, 21]. During NFκB signaling, the protein RIPK1 is attached to the membranous TNFR and is ubiquitinated by LUBAC and cIAP1

(Figure 3). During this time, the caspase-8 heterodimer cleaves a protein called CYLD which deubiquitinates RIPK1. If caspase-8 is downregulated or mutated in a nonfunctional manner, CYLD will deubiquitinate RIPK1 allowing for the phosphorylation of the protein RIPK3. RIPK3 will phosphorylate other downstream targets to cause necroptosis, or programmed necrosis, a cellular event that wasn't though to exist until caspase-8 knockouts [22]. It has also been determined that the cleavage of the intersubunit linker in the heterodimer has an impact on substrate preference and possibly enzyme stability. A cleaved caspase-8 within the caspase-8-FLIP heterodimer causes more NFκB activation than an uncleavable caspase-8 mutant [23].

E. Protein folding

Protein folding has many uses ranging from simply determining if a protein is folded before an experiment to discovering an allosteric site in a protein and how that site effects its interactions with other proteins. While the structures of nearly 100,000 proteins are known, the pathways by which these proteins attain their native conformation remain largely undefined. Since Anfinsen's classic experiments on the folding of ribonuclease, we are still unable to predict a protein's structure based on its amino acid sequence. Furthermore, Levinthal's paradox has postulated that given the degrees of freedom of a peptide, it would require an impossible amount of time for a protein to reach its native form; a process we know that can take less than a second.

E.1. Energy landscapes and folding states

Under normal cellular conditions, proteins exist in equilibrium between folded and unfolded ensembles of states. An ensemble of states results from the energy landscape of the

protein. The folding pathway refers to the ensemble of states through which the peptide must pass to attain the native folded state. Because of the energy landscape and the nature of thermodynamics, the unfolding pathway is typically the reverse of the folding pathway. For some proteins however, this is not the case and the unfolding pathway is not the reverse which means there is a hysteresis in the folding pathway. A hysteresis occurs mainly in proteins that are multimeric or dimeric, such as caspase-3 [24], and is caused by high kinetic barriers to proper folding which is coupled to dimerization. While rare in monomeric folding, hysteresis can be caused by multiple energetic basins in the energy landscape with slow kinetics [25].

E.2. Thermodynamic and kinetic folding

In order to study the complete folding of a protein, one must study both the thermodynamic stability and the kinetic folding rates of the entire protein. If a protein contains multiple domains, it is necessary to study each domain separately and together for a complete picture of how the domains interact to stabilize each other [26]. In particular if a domain is not soluble, it is likely that there are extensive interdomain interfaces. Multiple domains may also present the interface between them an important factor in reaching and maintaining the native folded state. Interdomain interactions affect both the rate and stability of protein folding. Neighboring protein domains fold in a couple of different ways that make studying multidomain proteins challenging. First, protein domains fold off the ribosome co-translationally, one at a time, during synthesis of the protein from the mature RNA transcript. Second, domains will eventually unfold and then spontaneously refold during the lifetime of the protein.

Thermodynamic folding measures the stability of a protein and is given as $\Delta G_{D\text{-}N}$, that is the free energy of folding. The free energy of folding, or Gibb's free energy, is the difference between the energy of the denatured (nonspecifically collapsed) and native state. A protein folds simply because its native state is significantly lower in free energy than its denatured state. However, proteins are so stable that they fold once and remain that way until they are no longer needed. Proteins fold spontaneously after coming off of the ribosome and then naturally fall apart and subsequently refold. A typical protein can unfold every few minutes. The marginal stability allows for the fine tuning of protein function by keeping the folding energy near the boundary of unfolding. Furthermore, small changes in protein sequence can make the free energy of the folded state slightly higher than the unfolded state which would cause the protein to no longer fold properly. Kinetic folding measures the rate of folding and unfolding to elucidate how a protein gets from the denatured state to the native state. Understanding the folding mechanism and measuring the stability of mutations is imperative to the function of the protein.

E.3. Protein folding among homologous proteins

Cytochrome C folds 1 million times faster than acylphosphatase [27]. This statement reflects how dynamic protein folding is. Anfinsen postulated that protein folding is spontaneous and also that a protein's primary sequence determines both structure and folding rate [28]. Therefore, a protein's primary sequence defines stability, structure, folding rate, and size. A two state folding model is the most basic of folding models and only involves a folded and unfolded state. The vast majority of single domain proteins fold in this manner. There is also a relation between sequence and folding kinetics, for example, there is a

statistically significant correlation between sequence identity and folding kinetics for homologous, single domain proteins ($r = .72$). It has been determined that protein folding rates are relatively insensitive to small changes in sequence as long as native structure and stability are maintained. For example, the folding rate of eight homologous sets of two proteins have been reported with a 53 – 86% sequence identity show only a modest difference in folding rate (< 15 fold) [29-36].

REFERENCES

1. Yu, J.W., P.D. Jeffrey, and Y. Shi, *Mechanism of procaspase-8 activation by c-FLIPL.* Proc Natl Acad Sci U S A, 2009. **106**(20): p. 8169-74.
2. Pop, C., et al., *FLIP(L) induces caspase 8 activity in the absence of interdomain caspase 8 cleavage and alters substrate specificity.* Biochem J, 2011. **433**(3): p. 447-57.
3. David W. Chang, Z.X., Yi Pan, Alicia Algeciras-Schimnich, Bryan C. Barnhart, Shoshanit Yaish-Ohad, Marcus E. Peter, and Xiaolu Yang, *c-FLIPL is a dual function regulator for caspase-8 activation and CD95-mediated apoptosis.* EMBO J, 2002. **21**(14): p. 3704-3714.
4. Ma, C., S.H. Mackenzie, and A.C. Clark, *Redesigning the procaspase-8 dimer interface for improved dimerization.* Protein Sci, 2014.
5. Tracey, D., et al., *Tumor necrosis factor antagonist mechanisms of action: a comprehensive review.* Pharmacol Ther, 2008. **117**(2): p. 244-79.
6. Micheau, O. and J. Tschopp, *Induction of TNF Receptor I-Mediated Apoptosis via Two Sequential Signaling Complexes.* Cell, 2003. **114**(2): p. 181-190.
7. Muzio, M., *An Induced Proximity Model for Caspase-8 Activation.* Journal of Biological Chemistry, 1998. **273**(5): p. 2926-2930.
8. Stennicke, H.R., *Pro-caspase-3 Is a Major Physiologic Target of Caspase-8.* Journal of Biological Chemistry, 1998. **273**(42): p. 27084-27090.

9. Jan Paul Medema, C.S., et al., *FLICE is activated by association with the CD95 death-inducing signaling complex (DISC).* EMBO J, 1997. **16**(10): p. 2794-2802.

10. Mielgo, A., et al., *Paclitaxel promotes a caspase 8-mediated apoptosis through death effector domain association with microtubules.* Oncogene, 2009. **28**(40): p. 3551-62.

11. Gonzalvez, F., et al., *TRAF2 Sets a threshold for extrinsic apoptosis by tagging caspase-8 with a ubiquitin shutoff timer.* Mol Cell, 2012. **48**(6): p. 888-99.

12. Dillon, C.P., et al., *Survival function of the FADD-CASPASE-8-cFLIP(L) complex.* Cell Rep, 2012. **1**(5): p. 401-7.

13. Beaudouin, J., et al., *Caspase-8 cleaves its substrates from the plasma membrane upon CD95-induced apoptosis.* Cell Death Differ, 2013. **20**(4): p. 599-610.

14. Ando, M., et al., *Cancer-associated missense mutations of caspase-8 activate nuclear factor-kappaB signaling.* Cancer Sci, 2013. **104**(8): p. 1002-8.

15. Honglin Li, H.Z., Chi-jie Xu, and Junying Yuan, *Cleavage of BID by Caspase 8 Mediates the Mitochondrial Damage in the Fas Pathway of Apoptosis.* Cell, 1998. **94**: p. 491–501.

16. Datta, S.R., et al., *Akt phosphorylation of BAD couples survival signals to the cell-intrinsic death machinery.* Cell, 1997. **91**(2): p. 231-41.

17. Srinivasula, S.M., et al., *A conserved XIAP-interaction motif in caspase-9 and Smac/DIABLO regulates caspase activity and apoptosis.* Nature, 2001. **410**(6824): p. 112-6.

18. Vallabhapurapu, S. and M. Karin, *Regulation and function of NF-kappaB transcription factors in the immune system.* Annu Rev Immunol, 2009. **27**: p. 693-733.

19. van Raam, B.J. and G.S. Salvesen, *Proliferative versus apoptotic functions of caspase-8 Hetero or homo: the caspase-8 dimer controls cell fate.* Biochim Biophys Acta, 2012. **1824**(1): p. 113-22.

20. Salmena, L. and R. Hakem, *Caspase-8 deficiency in T cells leads to a lethal lymphoinfiltrative immune disorder.* J Exp Med, 2005. **202**(6): p. 727-32.

21. Leverrier, S., G.S. Salvesen, and C.M. Walsh, *Enzymatically active single chain caspase-8 maintains T-cell survival during clonal expansion.* Cell Death Differ, 2011. **18**(1): p. 90-8.

22. O'Donnell, M.A., et al., *Caspase 8 inhibits programmed necrosis by processing CYLD.* Nat Cell Biol, 2011. **13**(12): p. 1437-42.

23. Micheau, O., et al., *The long form of FLIP is an activator of caspase-8 at the Fas death-inducing signaling complex.* J Biol Chem, 2002. **277**(47): p. 45162-71.

24. Mackenzie, S.H. and A.C. Clark, *Slow folding and assembly of a procaspase-3 interface variant.* Biochemistry, 2013. **52**(20): p. 3415-27.

25. Sambrook, M.J.G.a.J., *Protein folding in the cell.* Nature, 1992. **355**(12): p. 31-47.

26. Han, J.H., et al., *The folding and evolution of multidomain proteins.* Nat Rev Mol Cell Biol, 2007. **8**(4): p. 319-30.

27. Wittung-Stafshede, P., et al., *Cytochrome b562 folding triggered by electron transfer: approaching the speed limit for formation of a four-helix-bundle protein.* Proc Natl Acad Sci U S A, 1999. **96**(12): p. 6587-90.

28. Anfinsen, C.B., *Principles that Govern the Folding of Protein Chains.* American association for the advancement of science, 1973. **181**(4096): p. 223-230.

29. David E. Kim, H., Gu, and David Baker, *The sequences of small proteins are not extensively optimized for rapid folding by natural selection.* Proc Natl Acad Sci U S A, 1998. **95**: p. 4982-4986.

30. Plaxco, K.W., et al., *Topology, stability, sequence, and length: defining the determinants of two-state protein folding kinetics.* Biochemistry, 2000. **39**(37): p. 11177-83.

31. Plaxco, K.W., K.T. Simons, and D. Baker, *Contact order, transition state placement and the refolding rates of single domain proteins.* J Mol Biol, 1998. **277**(4): p. 985-94.

32. Reid, K.L., et al., *Stability and folding properties of a model beta-sheet protein, Escherichia coli CspA.* Protein Sci, 1998. **7**(2): p. 470-9.

33. Perl, D., et al., *Conservation of rapid two-state folding in mesophilic, thermophilic and hyperthermophilic cold shock proteins.* Nat Struct Biol, 1998. **5**(3): p. 229-35.

34. Taddei, N., et al., *Thermodynamics and kinetics of folding of common-type acylphosphatase: comparison to the highly homologous muscle isoenzyme.* Biochemistry, 1999. **38**(7): p. 2135-42.

35. PG Wolnynes, J.O., *Fast-folding eriments and the topography of protein folding energy landscapes.* Chemistry & Biology, 1996. **3**: p. 425-492.

36. Plaxco, K.W., et al., *Rapid refolding of a proline-rich all-beta-sheet fibronectin type III module.* Proc Natl Acad Sci U S A, 1996. **93**(20): p. 10703-6.

FIGURES

Figure 1. Caspase classification. Initiator caspases are the apical caspases in the apoptotic pathway and are required for the activation of executioner caspases. Initiator caspases are limited in their dimer form to self-cleavage, Bid, and executioner caspases. They contain a recruitment pro-domain to allow for receptor recruitment and subsequent dimerization. Executioner caspases exist in cells as latent dimers and only require cleavage for their activation. Executioners of apoptosis cleave hundreds of substrates and are the responsible for the large phenotypic changes of apoptosis such as membrane blebbing and nuclear condensation. Taken from Green, (2010) Nature Reviews Molecular Cell Biology, 78, 225-231.

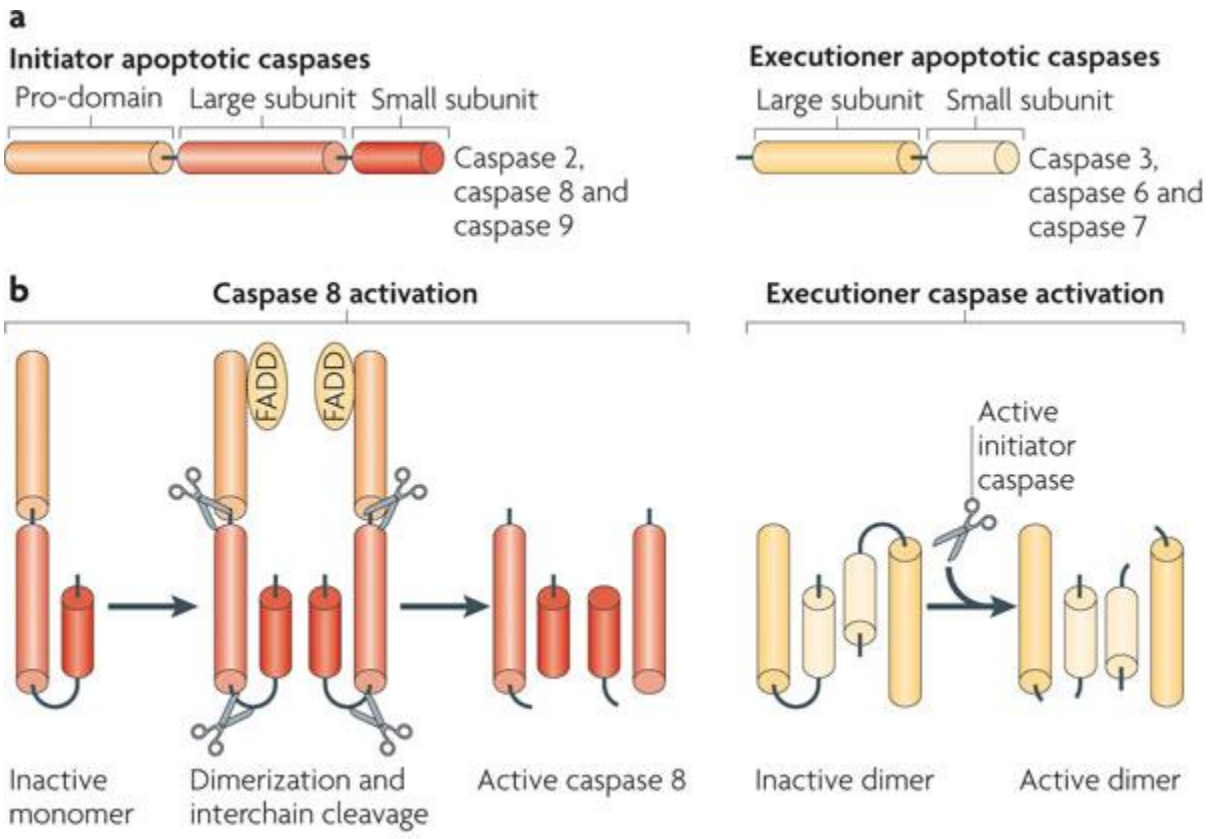

Nature Reviews | Molecular Cell Biology

Figure 2. Extrinsic and Intrinsic apoptotic pathways. In the extrinsic pathway, a death ligand (CD95L) binds to a death receptor (CD95), which signals adaptor proteins to bind to the receptor via homotypic death domain (DD) interactions. The adaptor protein interacts with the death effector domain (DED) of procaspases–2, –8, and –10, forming an activation complex called the DISC. Dimerization of caspase-8 results in maturation and full activity. Caspases–8 and –10 then process effector caspases. In the intrinsic apoptotic pathway, pore formation in the mitochondria, resulting from cleavage of Bid by caspase-8, reactive oxygen species (ROS), chemotherapeutic agents or p53, leads to a release of many pro-apoptotic factors; SMAC, cytochrome C, etc. Cytochrome C causes the formation of the apoptosome (red and pink). The apoptosome is composed of Apaf-1 monomers that form a heptameric structure when cytochrome c binds leading to interactions with the caspase recruitment domain (CARD) of procaspase–9. The interactions increase the local concentration of procaspase–9 monomers and thereby promote dimerization and activation. Caspase–9 then processes effector caspase-3, which leads to apoptosis. Inhibitors of apoptosis (IAPs), specifically XIAP, inhibit mature initiator or effector caspases (caspases –9, –3, and –7), and are inhibited by SMAC or DIABLO. Taken from Oberst, Green, (2011) Nature Reviews Molecular Cell Biology, 82, 341-364.

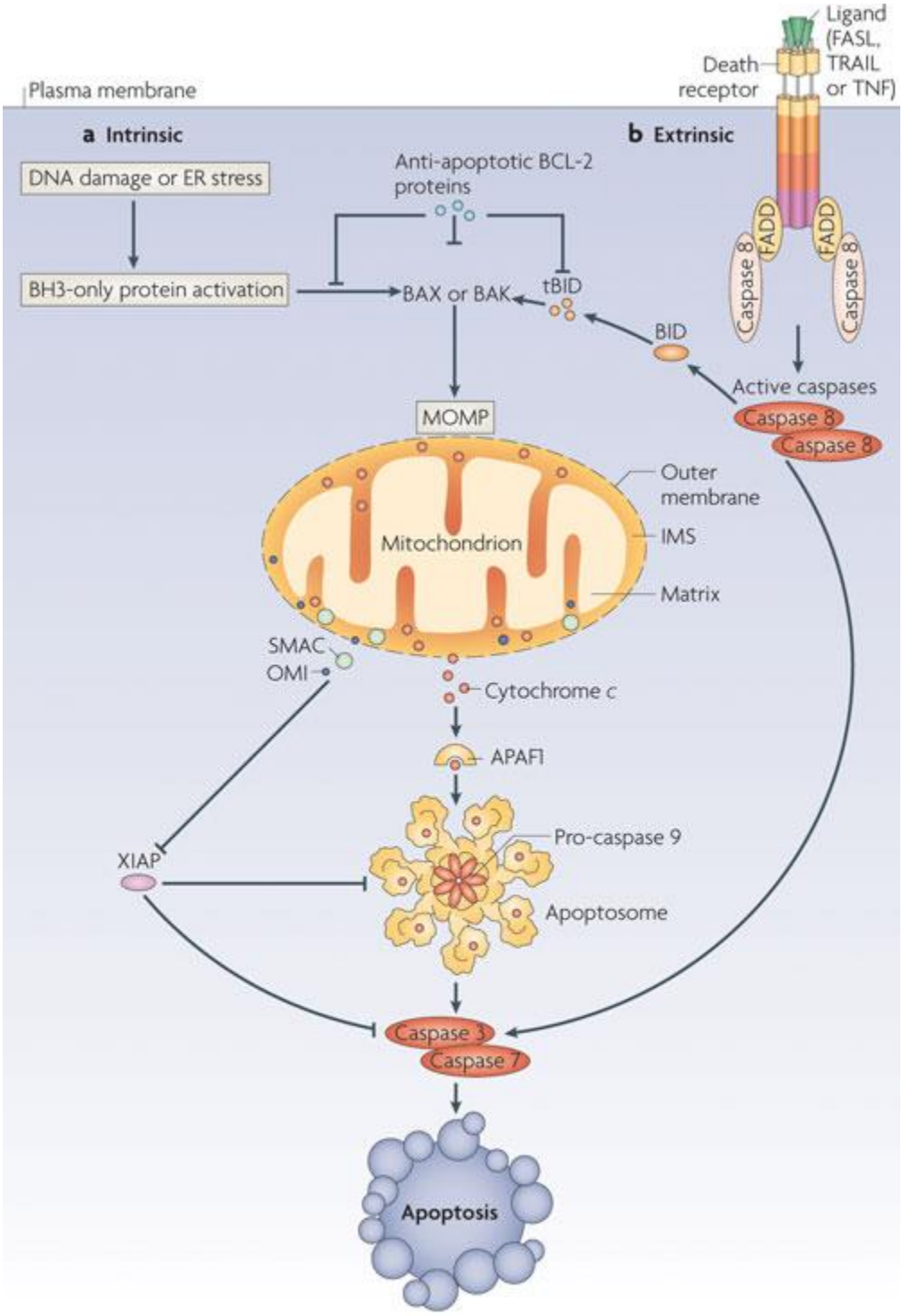

Nature Reviews | Molecular Cell Biology

Figure 3. Caspase-8 non-apoptotic functions. Caspase-8 can homodimerize to cause apoptosis and heterodimerize with FLIP to cause cell survival by cleaving CYLD to inhibit RIPK1-dependent necroptosis and by cause NFκB activation. TNFR1 ligation causes recruitment of RIPK1 and ubiquitination of RIPK1 in complex I. This formation causes NFκB activation which upregulates FLIP transcription. RIPK1 is then deubiquitinated and forms complex II in the cytosol with caspase-8 and FLIP dependent upon their cellular concentrations. Complex II can take three different directions: Survival by the action of the RIPK1-caspase-8-FLIP heterodimer, apoptosis by the action of the RIPK1-caspase-8 homodimer, and programmed necrosis (necroptosis) by the absence of caspase-8 which causes phosphorylation and activation of RIPK3. FLIP keeps apoptosis in check by binding caspase-8 monomers thereby causing survival and NFκB activation. FLIP also keep necroptosis from occurring by binding caspase-8 monomers and cleaving CYLD. Taken from Oberst, Green, (2011) Nature Reviews Molecular Cell Biology, 12, 757-763.

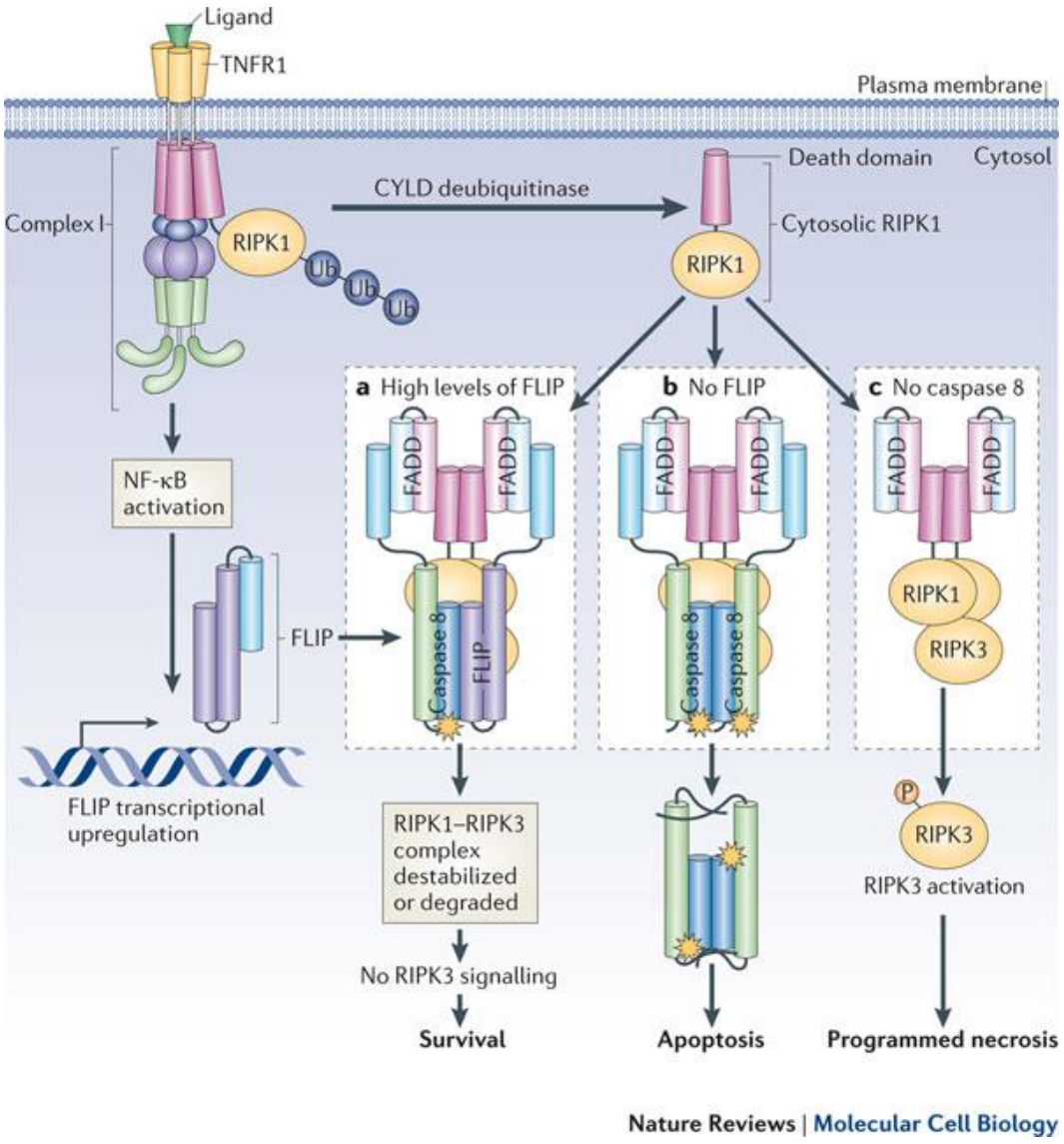
Ligand
TNFR1
Plasma membrane
Death domain
Cytosol
CYLD deubiquitinase
Complex I
RIPK1
Ub
Ub
Ub
Cytosolic RIPK1
RIPK1
a High levels of FLIP
b No FLIP
c No caspase 8
NF-κB activation
FADD
FADD
FLIP
Caspase-8
FLIP
Caspase-8
Caspase-8
RIPK1
RIPK3
FLIP transcriptional upregulation
RIPK1–RIPK3 complex destabilized or degraded
P
RIPK3
RIPK3 activation
No RIPK3 signalling
Survival
Apoptosis
Programmed necrosis
Nature Reviews | Molecular Cell Biology

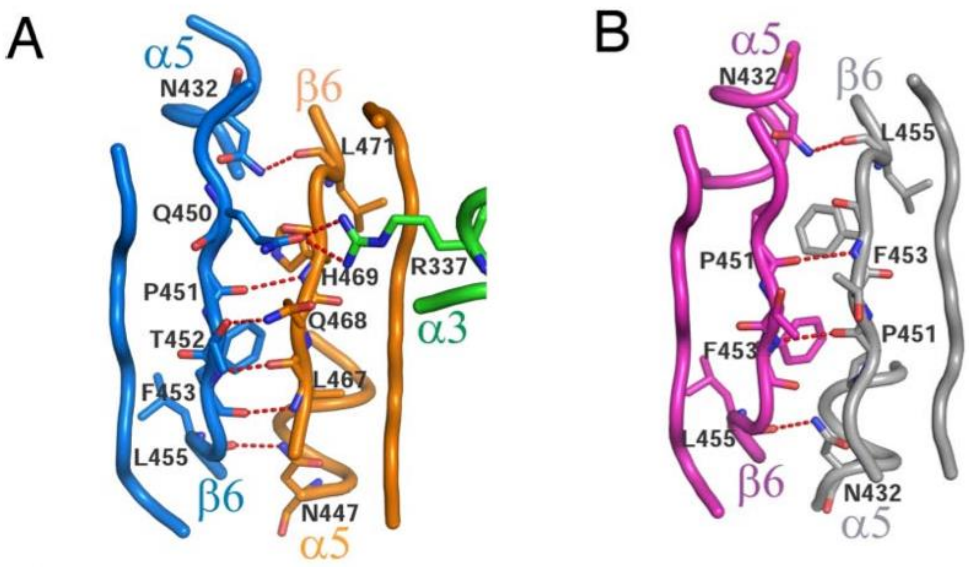

Figure 4. A: The caspase-8 (blue) and FLIP (orange and green) heterodimeric interface contains a network of hydrogen bonds. The hydrogen bonds are also shorter that those in the caspase-8 dimer interface. B: The caspase-8 dimer interface contains a suboptimal hydrogen bond network and negative design elements which create a low propensity for homodimer formation. Taken from Yu *et al*, (2009) Proc Natl Acad Sci, 19, 8169-8174.

CHAPTER II

Materials and Methods

Materials

Urea was purchased from ICN. Sodium citrate, tryptone, and ethanol were purchased from EMD. Yeast extract was purchased from BD Sciences. Sodium chloride, ampicillin sodium salt, acryladime, TEMED, potassium phosphate mono basic and dibasic were purchased from Fisher Science. HEPES, nickel sulfate, and imidazole were purchased from Acros. IPTG and DTT were purchased from Gold Biotechnology. The EDTA was purchased from EM Science. TRIS was purchased from JT Baker Sciences. The His-bind resin and Q-sepharose resin were purchased from VWR.

Stock Solutions

10 M Urea stock was prepared in 20mM phosphate buffer (pH 7.5) as described previously The molarity of prepared urea was determined by molecular weight measurement and confirmed by refractive index. 10 M urea stock solutions were prepared fresh for each experiment and were filtered prior to use with a 0.45μm filter.

Methods

A. Protein Purification

All steps were performed at 4 °C unless otherwise noted. DED-less Procaspase-8 was purified as a N-terminal-(His)7-tagged protein from *E. coli* BL21 (DE3) Plys S cells. FLIP(L) was purified as an N-terminal-(His)8-tagged protein from *E. coli* BL21 (DE3) Plys S cells and was a gift from Dr. Guy Salvesen. The DED-less procaspase-8 purification was modified from [1]. The DED-less FLIP purification was modified from [2]. The purification of both proteins was identical except for the IPTG concentration and induction time used to induce protein expression. An overnight culture was grown containing 100 mL of sterile LB,

50 ug/mL ampicillin, and a single plated colony at 37 °C. The amount of starter culture used to inoculate 1 L of sterile LB media using equation 1 depended upon the optical density at 600 nm (OD_{600}). This was typically 8 mL for FLIP and 9 mL for DED-less D_2A caspase-8. Cells were grown in Fernbach flasks which contained 1 L of sterile LB with 50 ug/mL ampicillin at 37 °C. When the cultures reached an OD_{600} of .6 for FLIP and .6 for caspase-8, expression of the promoter was induced with an IPTG final concentration of .1 mM for FLIP and .8 mM for caspase-8. The temperature was reduced from 37 °C to 25 °C for both proteins upon induction. The cells were allowed to induce overnight for FLIP and 9 hours for caspase-8. The cells were then harvested by centrifugation at 5000 rpm for 15 minutes and were stored at - 80 °C if needed. The cells were then resuspended in buffer A (50 mM Tris, 100 mM NaCl pH 8.0) and lysed via French press at 1100 PSI. The lysate was centrifuged at 14000 rpm for 45 minutes to separate the soluble protein from the insoluble fraction. The protein was first purified with a histidine affinity column which was equilibrated with buffer A. The supernatant from French press was poured over the column and then the column was washed with 200 mL of buffer B (50 mM Tris, 500 mM NaCl pH 8.0) and finally eluted with 50 mL of buffer C (50 mM Tris, 100 mM NaCl, 200 mM Imidizole pH 8). The protein was then dialyzed overnight against 50 mM Tris, 50 mM NaCl pH 7.9 supplemented with 1 mM DTT. The second purification step uses a Q-Sepharose column to further purify the protein to 95 % + purity. The dialyzed protein was poured over the column which was eluted with a salt gradient from 50 – 300 mM NaCl, 50 mM Tris pH 7.9 supplemented with 1 mM DTT. Fractions were collected and tests for protein content by a Bradford assay. Protein positive fractions were analyzed by SDS-PAGE (10-20 % gradient gels). The protein fractions were

combined and concentrated by Amicon N_2 filtration (YM 10 membrane). The concentrated protein was then dialyzed against 20 mM potassium phosphate buffer pH 7.5. The protein was stored at -20 °C. The concentrations of protein were found by using the ε280 of 23380 M^{-1} cm^{-1} for caspase-8 and 34880 M^{-1} cm^{-1} for FLIP.

B. Equilibrium unfolding

Equilibrium unfolding experiments were performed by mixing native protein with urea containing potassium phosphate buffer (20 mM KH2PO4/K2HPO4 pH 7.5) as described previously [3]. The final protein concentrations were 0.5, 1, 2, and 4 uM to examine concentration dependence. A quartz cuvette with a 1 cm path length was used for data collection. The fluorescence emission was measured from 300 to 400 nm following 280 and 295 nm excitation from 0 to 8 M urea in 0.25 M increments. This was set up using table 1 by preparing a stock solution of 0 M and 8 M urea solution which also contained 20 mM potassium phosphate buffer and 1 mM DTT. Each stock contained the respective amount of protein to equal 0.5, 1, 2, or 4 uM. The two stocks were pipetted by hand in ratios that gave 0 to 8 M urea, for example if a 2 M stock of urea was needed for a 1000 uL sample, 250 uL of 0 M and 750 uL of 8 M stock solution were combined into a microfuge tube.
Because each stock solution contains the same protein, DTT, and potassium phosphate concentrations, the stocks could be mixed in ratios. This eliminated the need to add a single amount of protein and DTT separately to each of the 33 tubes which greatly reduced hand pipetting error. The 33 samples that represent 0 to 8 M urea in .25 M increments were vortexed briefly to mix each sample before the samples were allowed to equilibrate overnight

in a 25 °C water bath. In control experiments, simply the stock solutions of 0 and 8 M urea were used.

B1. Data analysis

The raw emission spectra were plotted for each urea concentration to determine a shift toward increased or decreased wavelength. All measurements were corrected for buffer and machine noise. It is understood that once the core of a protein is unfolded, the emission spectra will shift to higher wavelengths. In contrast, the folding of a protein will shift to lower wavelengths. This is due to the aromatic residues tryptophan and phenylalanine at 280 or tryptophan alone at 295 nm excitations. Tryptophan in water emits at 350 nm while a buried tryptophan in the core of a protein emits at around 330-335. As the protein unfolds in higher and higher urea concentrations, residues will become more and more solvent exposed in a similar situation to the tryptophan in water example. In order to view the data and limit machine noise, it is necessary to take the average emission wavelength of each spectrum and plot it versus urea concentration. The average emission wavelength formula is shown below:

$$\lambda = \frac{\sum_{i=1}^{N}(I_i\lambda_i)}{\sum_{i=1}^{N}(I_i)}$$

where I is the intensity and λ is the wavelength.

The data were averaged for all data and fit globally to a two-state equilibrium folding process [4] using the programming language python and a scientific library called SciPy. Equation 1 defines how delta G and m-values are determined from fluorescence data.

$$N \overset{K_{Eq}}{\rightleftarrows} U \tag{1}$$

In this model, N represents the native monomer cooperatively unfolding to the unfolded protein U. The equilibrium constant for the reaction is given above the double headed arrow. The total molar concentration for the entire reaction is given in Equation 2.

$$P_T = [\mathrm{N}] + [\mathrm{U}] \tag{2}$$

The molar fraction of each state is defined in equations 3 and 4.

$$f_N = \frac{1}{1+K} \tag{3}$$

$$f_U = \frac{K}{1+K} \tag{4}$$

The sum of the molar fraction is equal to unity as shown in equation 5.

$$f_U + f_N = 1 \tag{5}$$

The equilibrium constant, K, is related to the mole fraction of each state and the total molar concentration as described by equation 6.

$$K_{eq} = \frac{f_U}{f_N} \tag{6}$$

The equilibrium constant definition can be substituted in terms of the molar fractions to yield equations 7 and 8.

$$f_N = \frac{N}{P_T} \tag{7}$$

$$f_U = \frac{U}{P_T} \tag{8}$$

The equilibrium constant for the transition from folded to unfolded state is given by the free energy as defined in equation 9.

$$\Delta G = \Delta G^{HOH} + RT \ln K \therefore \Delta G^{HOH} = -RT \ln K \quad (9)$$

R is the gas constant in cal K^{-1} mol^{-1} and T is in Kelvin. Free energy change of the reaction changes linearly with denaturant concentration; therefore the free energy change in the absence of urea is shown in equation 10. In equilibrium, delta G is 0.

$$\Delta G = \Delta G^{HOH} - m[urea] \quad (10)$$

where delta G water is the free energy change in the absence of urea and m1 represents the cooperatively index of the reaction. The amplitude of the intrinsic fluorescence signal measured at each urea concentrations represented by a linear combination of the fractional contribution from each state is given in equation 11.

$$Y = Y_N f_N + Y_U f_U \quad (11)$$

where Y_N and Y_U represent the signal of the native and unfolded states respectively, in the absence of urea. The amplitudes of the native and unfolded states of the protein are also assumed to be linearly dependent with urea concentration as described in equations 12 and 13.

$$Y_N = Y_{N'} + m_3[urea] \quad (12)$$

$$Y_U = Y_{U'} + m_2[urea] \quad (13)$$

where Y native prime and Y unfolded prime are the amplitudes of the intrinsic fluorescence signal in the absence of urea. Solving for Y and taking into account equations 12 and 13, one can solve for the fitting model described in equation 14 which is trained to sets of equilibrium folding data.

$$Y = Y_N F_N + Y_U F_U = \frac{\left((Y_N + m_N[urea]) + (Y_U + m_U[urea])((e^{-\Delta G^{HOH} - m[urea]})/(RT))\right)}{1 + \left((e^{-\Delta G^{HOH} - m[urea]})/(RT)\right)} \quad (14)$$

where the m-native and m-unfolded are slopes for the signal in the pre-transition and post-transition as the urea concentration increases. The Y-native prime and Y-unfolded prime values represent the signal of the folded and unfolded states in the absence of urea. Inherent to equation 14 is the sum of the fractional states (folded and unfolded) is represented by the intrinsic fluorescence signal.

Equation 14 is used to describe the two-state model for equilibrium unfolding of a monomer. This is the simplest case for protein folding as a three and four state folding model have been described previously [5].

B2. Fitting equilibrium unfolding data

There are many graphing programs available for fitting data to a model. Kaleidograph and Igor pro have been described previously [6]. Here, I describe a way to train the model in equation 14 globally to data. The data must be fit globally in order to obtain a more concise fit where delta G and m are linked among all sets of data and the Y-native and Y-unfolded are set locally because they vary for each set. Python has been used for scientific data analysis for the last decade and runs programs such as Pymol. Python also contains a wide array of commonly used scientific libraries such as SciPy, NumPy, and Biopython which are used in the construction of Pymol. The code I have written uses the libraries SciPy and NumPy to optimize the non-linear least squares fit of the data sets using Python 2.7.5. The

IDE used to write and compile the code was IDLE. All data sets and the working python file must be in the same directory. The two-state fitting program is shown below:

```
from pylab import *
from scipy.optimize import leastsq
import csv

data = [] # Put data here
with open('Data.csv', 'rb') as csvfile:
    datareader = csv.reader(csvfile, delimiter=',')
    datareader.next()
    data = array(list(map(float, row) for row in datareader))

average = data[:, 9]
urea_conc = data[:, 0]

def residuals(p):
   # Calculates error
   return six_term_model(urea_conc, p)-average

def six_term_model(urea, p):
   y_f, m_f, y_u, m_u, m, dG = p
   RT = 0.5862
   numerator = (y_f + m_f*urea) + (y_u + m_u*urea)*exp((-dG-m*urea))/RT
   denomenator = 1 + exp((-dG-m*urea))/RT
   return numerator / denomenator

p0 = [342.5, 4, 350, 4, 1, -4]

fitted_params = leastsq(residuals, p0)[0]
fig = figure()
ax = fig.add_subplot(111)
plt.title('Two state folding model')
plt.xlabel('[urea] M')
plt.ylabel('Average Emission Wavelength')
ax.plot(urea_conc, data[:, 1], '.')
ax.plot(urea_conc, data[:, 2], '.')
ax.plot(urea_conc, data[:, 3], '.')
ax.plot(urea_conc, data[:, 4], '.')
ax.plot(urea_conc, six_term_model(urea_conc, fitted_params), 'ko-')
print fitted_params
show()
```

The three-state fitting program uses the same logic to handle the data and turn it into an array. The definition of the model has changed to reflect that of the three-state folding model described in [6]. The source code is shown below:

```
from pylab import *
from scipy.optimize import leastsq
import csv

data = [] # Put data here
with open('Data.csv', 'rb') as csvfile:
    datareader = csv.reader(csvfile, delimiter=',')
    datareader.next()
    data = array(list(map(float, row) for row in datareader))

average = data[:, 9]
urea_conc = data[:, 0]

def residuals(p):
   # Calculates error
   return eight_term_model(urea_conc, p)-average

def eight_term_model(urea, p):
   dG1, m1, dG2, m2, Yf, mf, Yu, mu, Yi = p
   RT = .5802
   K1 = exp(-((dG1+m1*urea)/(RT)))
   K2 = exp(-((dG2+m2*urea)/(RT)))
   Ff = 1/(1+K1+K1*K2)
   Fi = K1/(1+K1+K1*K2)
   Fu = (K1*K2)/(1+K1+K1*K2)
   Y1 = Yf+mf*urea
   Y2 = Yu+mu*urea
   y = Y1*Ff+Yi*Fi+Y2*Fu
   return y

p0 = [1.03, -1, 4, -.5, 345.6, 1, 344.3, .5, 343.3]

fitted_params = leastsq(residuals, p0) [0]
fig = figure()
ax = fig.add_subplot(111)
plt.title('Three state folding model')
plt.xlabel('[urea] M')
```

```
plt.ylabel('Average Emission Wavelength')
ax.plot(urea_conc, data[:, 1], '.')
ax.plot(urea_conc, data[:, 2], '.')
ax.plot(urea_conc, data[:, 3], '.')
ax.plot(urea_conc, data[:, 4], '.')
ax.plot(urea_conc, six_term_model(urea_conc, fitted_params), 'ko-')
print fitted_params
show()
```

C. Circular Dichroism

Circular dichroism experiments were performed in conjunction with intrinsic fluorescence to examine secondary and tertiary structure data for unfolding. A PiStar spectrophotometer from applied photo physics was used for near and far UV experiments. DED-less D2A procaspase-8 was used at 10 uM in all experiments. Native protein in 20 mM potassium phosphate buffer pH 7.5, .1 mM DTT was hand mixed with a 9 M urea containing potassium phosphate buffer pH 7.5 to obtain 0, 4, and 8 M urea final concentrations. The solutions were allowed to sit overnight in a 25 °C water bath to allow for equilibrium. The spectrum was measured at far UV (190-250 nm) and near UV (250-320 nm). To avoid amplification of the high tension voltage in high urea concentrations, the signal was monitored at 228 nm for secondary structure. The urea concentrations were chosen to verify the secondary and tertiary structure signal change upon denaturation and to compare the data to the intrinsic fluorescence data

D. Size Exclusion Chromatography

Size exclusion chromatography separates proteins based on their hydrodynamic volume which is interpreted to size. The Superdex 75 10/300 GL short gel column contains a

porous matrix of cross-linked agarose and dextran. The porosity of the beads allow small proteins to travel into small pores formed by the beads and keep larger proteins from entering the beads forcing them the travel around the pores. This principle infers that smaller proteins have longer retention times while larger proteins have shorter retention times and therefore elute first. To collect the eluted proteins, the column is attached to an AKTA FPLC (Amersham Biosciences, Piscatawat, NJ), which measures the absorbance at 280 nm of eluted proteins to determine the relative elution volumes of the sample proteins. The software that runs the program is the UNICORN suite which records and displays the absorbance peaks versus volume. This graph is called a chromatogram and is used to determine the approximate molecular weight of the sample dependent upon the standard curve defined by running standards over column.

D.1. Column Parameters and Calibration

The Superdex 75 10/300 GL has a separation range of 3000 to 75000 daltons and a size exclusion limit of 100000 daltons. The separation range is particularly useful for resolving and separating monomer from dimer. To distinguish the sizes of proteins, it is necessary to run numerous standardized, known proteins over the column. By determining the elution volumes of each known standard molecular weight, one can create a standard linear equation from the calibration curve. The elution profiles of Aprotinin (6500 Da), RNAse A (13700 Da), Carbonic Anhydrase (29000 Da), Ovalbumin (44000), and Conalbumin (75000) were determined. From the elution volumes, Kav values were determined from equation 1.

$$K_{av} = \frac{V_e - V_o}{V_c - V_o} \quad (1)$$

where V_o is the column void volume which is 24 mL, V_e is the elution volume of each sample, and V_c is the geometric column volume which is determined by the elution volume of Blue Dextran. Blue Dextran is far above the molecular weight cut off of the column and flows through the column rapidly. A calibration curve is then prepared by plotting the K_{av} values versus the log molecular weight of the samples. A linear fit of the curve was determined from the plot and is shown in equation 2.

$$y = -0.3601x + 1.8409 \quad (2)$$

In this equation, the molecular weight of a protein can be obtained by solving for x and setting y equal the K_{av} of the eluted protein. Instrument procedure has been described previously [7].

D.2. Sample Preparation

SEC was used to determine the oligomeric status of DED-less procaspase-8 D2A with DED-less FLIP at concentrations of urea that correspond to possible intermediary states for both proteins from the intrinsic fluorescence unfolding data. All samples were prepared in the same fashion. 0.5 mg/mL FLIP and 0.5 mg/mL procaspase-8 (total volume 1.2 mL) were dialyzed overnight in at least 20x (40 mL) the appropriate urea containing 20 mM potassium phosphate buffer pH 7.5 supplemented with 1 mM DTT. To limit crystal formation and allow for proper mixing, dialysis was performed by placing the sealed dialysis bag in a 50 mL

Falcon conical which was placed in a shaker at 150 rpm, 25 °C. Before injecting the protein onto the column, the dialysis bag contents were centrifuged at 13000 rpm to remove any debris. The resulting peak fraction was collected and stored at - 20 °C.

E. Kinetic Folding Studies

E.1. Single mixing stopped-flow fluorescence

Single mixing kinetic experiments were performed using a stopped-flow spectrofluorometer (SX18) from Applied Photophysics. The temperature was kept constant by using a circulating water bath at 25 °C. The samples were excited at 280 and 295 nm and fluorescence emission was measured using a 305 nm cut off filter. The slits were set to 0.76 mm, 2 mm, and 2 nm respectively.

The refolding experiments were performed by mixing unfolded protein at 22 uM in 8 M urea and 20 mM potassium phosphate buffer pH 7.5. The final concentration of protein was 2 uM.

E.2. Measuring folding kinetics

Experimental procedures and initial instrument parameterization and procedures and protocols for single-mixing stopped-flow kinetics have been described in detail previously [6].

E.3. Data Analysis

Determining the number of phases is the first step in analyzing kinetic folding data. A phase is defined as any spectroscopic signal dependent change over time and is described by

a change in amplitude in the case of a burst phase or a single rate constant. This is determined by plotting the signal versus time in seconds.

F. Caspase-8 dimerization assay

Procaspase-8 D2A was dimerized by using a high concentration of the kosmotrope sodium citrate. As endogenous apical caspase zymogens are monomeric, the formation of the dimer will have a noticeable shift in the intrinsic fluorescence profile of the enzyme; similar to denaturation or renaturation but less dramatic. This is due to the single tryptophan near the active site of procaspase-8 and two tyrosine residues in proximity of the tryptophan. Upon dimerization, we hypothesized that the emission of the highly sensitive tryptophan residue would change based upon the environmental changes occurring due to dimerization.

Kosmotrope induced dimerization has been used previously to study caspases and sodium citrate was determined to cause the greatest amount of dimerization and activity measurements for caspase-8 [8]. The purpose of this assay was to determine if an average emission wavelength shift would occur upon dimerization and if so, how much.

DED-less procaspase-8 D2A at 1 uM was incubated in increasing concentrations of sodium citrate from 0 to 1 M sodium citrate in 0.1 M increments for 60 minutes in a 25 °C water bath. A quartz cuvette with a 1 cm path length was used for data collection. The fluorescence emission was measured from 300 to 400 nm following 280 and 295 nm excitation using a PTI spectrofluorometer. The slits used were 3 - 3 - 4 - 4.

REFERENCES

1. Pop, C., G.S. Salvesen, and F.L. Scott, *Chapter 21 Caspase Assays: Identifying Caspase Activity and Substrates In Vitro and In Vivo.* 2008. **446**: p. 351-367.
2. Pop, C., et al., *FLIP(L) induces caspase 8 activity in the absence of interdomain caspase 8 cleavage and alters substrate specificity.* Biochem J, 2011. **433**(3): p. 447-57.
3. Chen, Y.R. and A.C. Clark, *Kinetic traps in the folding/unfolding of procaspase-1 CARD domain.* Protein Sci, 2004. **13**(8): p. 2196-206.
4. Bolen, M.S.a.D.W., *Unfolding free energy changes determined by the linear extrapolation method. 1. Unfolding of phenylmethanesulfonyl alpha-chymotrypsin using different denaturants.* American Chemical Society, 1988. **442**: p. 123-132.
5. Walters, J., et al., *Allosteric modulation of caspase 3 through mutagenesis.* Biosci Rep, 2012. **32**(4): p. 401-11.
6. Walters, J., S.L. Milam, and A.C. Clark, *Chapter 1 Practical Approaches to Protein Folding and Assembly.* 2009. **455**: p. 1-39.
7. Mackenzie, S.H. and A.C. Clark, *Slow folding and assembly of a procaspase-3 interface variant.* Biochemistry, 2013. **52**(20): p. 3415-27.
8. Boatright, K.M., et al., *A unified model for apical caspase activation.* Mol Cell, 2003. **11**(2): p. 529-41.
9. Kelly M. BOATRIGHT, C.D., Jean-Bernard DENAULT, Daniel P. SUTHERLIN and Guy S. SALVESEN, *Activation of caspases-8 and -10 by $FLIP_{(L)}$.* Biochemistry, 2004. **382**: p. 651-657.

10. Pop, C., et al., *Role of proteolysis in caspase-8 activation and stabilization.* Biochemistry, 2007. **46**(14): p. 4398-407.

11. Yu, J.W., P.D. Jeffrey, and Y. Shi, *Mechanism of procaspase-8 activation by c-FLIPL.* Proc Natl Acad Sci U S A, 2009. **106**(20): p. 8169-74.

CHAPTER III

Results

A. Denaturation of DED-less procaspase-8 (D2A)

A.1. Intrinsic fluorescence

It has been established that procaspases cannot be purified in high concentrations in their full length form due to the insolubility of the pro domain. For this reason, the DED of procaspase-8 was not expressed, leaving only the catalytic domain. The catalytic domain of procaspase-8 contains two cleavage sites in the intersubunit linker at residues D374 and D384 which were mutated to alanine residues to prevent this cleavage. This keeps the large and small subunits intact during purification and experiments. We refer to this mutation as "D2A." The procaspase-8 construct used in all experiments was DED-less procaspase-8 D2A. Procaspase-8 contains one tryptophan residue near the active site of the protein (W420) and twelve tyrosine residues distributed within the primary structure. Therefore, fluorescence spectroscopy is a convenient and inexpensive technique to study the folding and unfolding of the tertiary structure. Excitation at 280 nm causes emission from both tyrosine and tryptophan residues, but the tyrosine residues in the vicinity of a tryptophan will transfer their energy to a neighboring tryptophan allowing us to study the environment of a tryptophan more closely. Excitation at 295 nm allows emission from only tryptophan residues.

The time required to obtain equilibrium from a folded to unfolded sample is determined as a baseline incubation time for all further experiments. Fluorescence emission scans for DED-less procaspase-8 D2A are shown in figure 1 after 280 nm excitation. The curve in red represents native protein and the other curves represent protein being denatured at various time points in 4 M urea. The native protein has a fluorescence maximum at 332 nm and after 8 hours of incubation, the 4 M urea curves have a maximum of 340 nm.

Fluorescence emission scans of the protein for 0 – 8 M urea in 1 M increments at an excitation of 280 nm is shown in figure 2 and an excitation of 295 nm in figure 3. Figures 2 and 3 show an average of three repeats but omit the error bars for clarity. Figure 4 shows the same data with error bars at 0 M and 8 M urea. The shift from the folded, native spectrum in red to the unfolded spectra in higher urea concentrations occurs because of solvent exposed tryptophan residues. As tryptophan residues become more solvent exposed, their emission shifts to higher wavelengths. Tryptophan in water emits at 353 nm representing the maximum wavelength. This shift is most clearly represented by the excitation at 295 nm data.

Each spectrum can be defined by a single point using the average emission wavelength equation which reduces machine noise and shows how the data shifts to higher wavelengths in higher urea concentrations. Average emission wavelength spectra for 280 and 295 excitations are shown in figures 5 and 6, respectively. In this data, the native protein has an average emission wavelength of 340 for 280 nm excitation and 342.4 nm for 295 nm excitation. The unfolded protein has a wavelength of 344 nm for 280 nm excitation and 350.5 nm for 295 nm excitation data. The $urea_{1/2}$ is 4 M and 5.2 M for 280 nm and 295 nm excitation, respectively.

A2. Reversibility of the procaspase-8 folding mechanism

To determine thermodynamic parameters from the unfolding of procaspase-8, the refolding curve must overlay with the data presented in figures 5 and 6. In order to determine if the unfolding pathway is reversible, that is, the folding pathway is the inverse of the unfolding pathway, intrinsic fluorescence was measured on unfolded protein which was diluted to lower and lower urea concentrations. Protein was denatured in 9 M urea and

allowed to equilibrate overnight. This denatured protein stock was then diluted from 9 M to 1 M urea in 1 M increments. These solutions were allowed to equilibrate overnight once again to reach equilibrium. The results are shown in figure 7 where the blue squares represent the refolding pathway and the red circles represent the unfolding pathway. Clearly, the unfolding pathway is reversible.

A3. Protein concentration dependence of the procaspase-8 folding mechanism

In order to determine if the folding of the monomer is a protein concentration dependent step, studying multiple concentrations of procaspase-8 was performed. Procaspase-8 unfolding was measured at 0.5, 1, 2, and 4 uM concentrations shown in figure 5 at 280 nm excitation and figure 6 at 295 nm excitation. These data show no protein concentration dependent change in signal. In addition, from these data, one can distinguish two states: the folded state at low wavelengths and the unfolded state at higher wavelengths. Furthermore, all of the protein concentrations can be fit together to the two state folding model. From this model, the thermodynamic parameters ΔG and the m-value can be determined. The average emission wavelength data for procaspase-8 was fit to a two-state folding model shown in figure 8 where the solid black line represents the fit. The thermodynamic parameters from the fitting model are shown in table 1. The free energy of folding in the absence of urea was determined to be 4.4711 kCal/mol. The m_f and m_U values describe how the folded and unfolded signal changes with urea concentration. The m-value relates to the cooperativity index which describes how the free energy changes with urea.

B. Denaturation of DED-less FLIP

B.1. FLIP contains an intermediate in its folding mechanism

FLIP is homologous to procaspase-8 but lacks the crucial residues necessary for enzyme activity. The protease domain of FLIP contains three tryptophan residues, W403, W453, and W466; and eleven tyrosine residues distributed throughout the primary structure of the protein. The tryptophan residues are not conserved between procaspase-8 and FLIP as shown in figure 9. W466 of FLIP is important in the stabilization of the active site of procaspase-8 in the heterodimer as it hydrogen bonds with R376 to keep the active site loops in a stable conformation allowing for the positioning of the catalytic cysteine (C345) of procaspase-8. For this reason, W466 is already in a fairly solvent exposed position compared to W403 which is buried in the monomeric form and switches conformations in the dimeric form of the protein (Figure 9B). Due to the extra tryptophan content and the proximity of the tyrosine residues to the tryptophans, the intrinsic fluorescence is much higher than that of procaspase-8 as shown in figures 10 and 11. The same experiments that were done on procaspase-8 were repeated with FLIP. The average emission wavelength of FLIP at 280 nm excitation and 295 excitation are shown in comparison to that of procaspase-8 in figures 12 and 13. In contrast to procaspase-8, FLIP appears to fold via a three-state mechanism. The pre-transition of the pathway has an average emission wavelength from 0 to 2 M urea while the post-transition occurs from 7 to 8 M. The first transition occurs from 2 to 3.25 M urea where the signal blue shifts to decreasing wavelengths corresponding to the compacting and internalizing of the aromatic residues in FLIP. Interestingly, there is an intermediate that occurs at wavelengths lower than that of the native state of the protein between urea

concentrations of 3.25 and 4.75 M. The signal then red shifts from 4 to 7 M urea to higher wavelengths corresponding the aromatic residues becoming more and more solvent exposed representing protein unfolding. The $urea_{1/2}$ is 6 M. At excitation of 295 nm, FLIP and procaspase-8 unfold to expose their tryptophan residues equally to solvent in 8 M urea (Figure 13). The higher average emission wavelengths in the native state of FLIP also confirm that the tryptophan residues are more solvent exposed compared to procaspase-8. The average emission wavelength measurements were repeated using multiple protein concentrations to determine if there is any protein concentration dependent change in the signal (Figure 14). The reversibility of the folding pathway is shown in figure 14 with the blue circles representing the refolding pathway from 8 to 1 M urea. Clearly, the unfolding pathway is reversible and not protein concentration dependent. Due to the unfolding pathway being reversible, one can fit the average emission wavelength spectrum to a three-state folding model (Figure 15). Thermodynamic parameters can be estimated from the model based on the data provided to the program for the free energy of folding in the absence of urea (ΔG^{HOH}) and the m-value for FLIP as shown in table 2.

C. Collapse of procaspase-8 secondary structure

The unfolding of procaspase-8 was monitored by circular dichroism in order to confirm the results seen in intrinsic fluorescence where tertiary structure was measured. The collapse of secondary and tertiary structure (not shown) was measured by far and near UV. An unfolding profile was generated by plotting the CD spectra at increasing urea concentrations. The unfolding profile at far UV depicts a loss of β-sheet content in urea concentrations greater than 4.25 M (Figure 16). No significant decrease in β-sheet content

occurred in urea concentrations less than 4.25 M. However, large decreases in overall secondary structure were observed in urea concentrations greater than 6 M. At 8 M urea, procaspase-8 still retains some of its secondary structure. In low urea concentrations, it appears that the beta sheet content is stabilized as evidenced by the decrease in molar ellipticity for 2 M urea.

D. Procaspase-8 refolding kinetics

Single mixing refolding studies were performed using stopped-flow fluorescence to determine a more complete picture of the procaspase-8 folding pathway. The intrinsic fluorescence data for procaspase-8 pointed to a possible intermediate in folding at an average wavelength of around 345 nm and 4.5 M urea. Stopped-flow fluorescence allows us to measure the tryptophan environment in a time-dependent manner on a millisecond scale. By measuring the environment of tryptophan, one can determine whether the protein in folded or unfolded by the solvent exposed nature of tryptophan. A solvent exposed tryptophan emits at lower intensity representing the unfolded state of the protein. A folded protein will shield the tryptophan from solvent allowing it to emit at higher wavelengths. Native procaspase-8 provides a baseline for where fluorescence signal should end upon refolding. Procaspase-8 incubated in 8 M urea overnight provides a starting signal for the unfolded protein's starting point in the refolding process. The mixing time of the stopped-flow fluorometer is approximately 1-2 milliseconds. During the mixing dead time, it is possible that the protein in question may fold which is referred as a "burst phase." It is also possible that a protein may have no signal change upon mixing for an extended period of time which is referred as a "lag phase."

D.1. Procaspase-8 contains a lag phase upon refolding

Stopped-flow fluorescence was measured at 1, 10, 100, and 1000 s time points to accurately determine whether intermediates exist in the folding pathway. The goal of this experiment was not to obtain microscopic rate constants from a chevron plot. The analysis of time dependent changes in signal show a lag phase in the first 60 seconds of refolding (figure 17), followed by an exponential growth phase, and an equilibrium phase which is not seen due to the limitation of our fluorometer. In order to view the equilibrium phase extrapolate to the final folded boundary, it will be necessary to lower the pH of the experiment or increase the temperature. No intermediate is present confirming the two phase equilibrium unfolding data.

E. FLIP refolding kinetics

The equilibrium unfolding of FLIP revealed an intermediate in the folding pathway. The pathway was further analyzed by measuring the fluorescence as the protein folds from an unfolded state to a folded state using a stopped-flow fluorometer in the same manner as procaspase-8 was analyzed.

E.1. FLIP folds faster than procaspase-8

Stopped-flow fluorescence was measured at 1, 10, 100, and 1000 s time points to examine the rate of the folding pathway in comparison to FLIP. In the plot showing the change in fluorescence in 1 second, the protein has obtained more than half of the native signal (figure 18). This rate contrasts vastly with procaspase-8 which was in a lag phase for a full 60 seconds. In measurements consisting of 100 s (figure 19), the signal contains a quick burst of folding as seen by the steep exponential phase followed by a relative flattening of the

signal and a second exponential growth phase. Albeit slightly slower than the first exponential phase, the second exponential phase reaches 85% of the way to the folded signal. Figure 20 depicts 1000 seconds of the refolding pathway and shows the signal equilibrate to the folded signal after 300 seconds. These data show an intermediate in the folding of FLIP and also that FLIP folds over 1000 seconds quicker than procaspase-8.

F. Kosmotrope induced dimerization of procaspase-8

Activity assays provide an easy and efficient way of testing the activity status of procaspase-8 during mutagenesis probing experiments but lack information as to how much mature caspase-8 dimer has formed relative to the monomer. For this reason, we sought a reliable method of examining the dimerization of procaspase-8. Kosmotropes have been used previously to dimerize procaspase-8. In order to determine how much dimer has formed, intrinsic fluorescence of procaspase-8 was measured to determine if there was a signal change that could be followed upon dimerization. Procaspase-8 was incubated in 0 – 1 M sodium citrate in 0.25 M increments for 1 hour before measurements were taken. From the raw fluorescence data (Figure 21), a change was seen in higher sodium citrate experiments where the amplitude of the emission curve increased with sodium citrate concentration. The shift in amplitude is most significant after .6 M sodium citrate. Average emission wavelengths were calculated from the raw data and three protein concentrations were tested (0.5, 1, and 2 uM) to determine if the signal was protein concentration dependent (Figure 22). The average emission wavelength data show an initial red shift to higher wavelengths in low sodium citrate concentrations (0.1 - .4 M) and then the data blue shifts sharply to lower wavelengths in higher concentration of sodium citrate (0.4 – 1 M). The red shift corresponds

to the aromatic residues becoming slightly exposed and the blue shift corresponds to the aromatics becoming more buried in the protein tertiary structure. As tryptophan is the primary residue emitting in the excitation wavelengths and the only tryptophan in the structure is on loop 2, it is likely that the loops are becoming more organized in high sodium citrate concentrations. The idea that loop rearrangements result from high sodium citrate concentrations was also stated in papers examining the kosmotrope dimerization effect on procaspase-8 dimerization [8-10].

G. The caspase-8-FLIP heterodimer folds by an intermediate in the FLIP folding pathway

Procaspase-8 exists in cells as a latent monomer and is able to homodimerize with another procaspase-8 monomer or heterodimerize with the homologous protein FLIP. Upon dimerization (hetero or homo) caspase-8 will cleave the intersubunit linker of FLIP and then its own intersubunit linker. The procaspase-8 variant used in all experiments has two mutations in the intersubunit linker rendering it incapable of being cleaved and DED-less. FLIP is absent the mutations and also DED-less rendering it cleavable upon heterodimerization with procaspase-8.

G1. Conditions of heterodimerization

The conditions we tested were based on the folding profiles of both procaspase-8 and FLIP. Procaspase-8 has a $urea_{1/2}$ of 4 M which means that there is a population of both unfolded and folded procaspase-8 at that urea concentration. FLIP has a semi-stable populated intermediate state at 4M urea. As previous research has shown that procaspase-8 and FLIP heterodimerize very poorly in their native conformations *in vitro* [11], we

hypothesized that the heterodimer may form more efficiently if the intermediate state of FLIP is populated in 4 M urea.

G.2. Multiple cleavage products of FLIP are observed upon heterodimerization

Procaspase-8 is 29.5 kDa in molecular weight and was resolved at 1 mg/mL on a sizing column (Figure 23). FLIP is slightly larger at 36 kDa and was resolved at 1 mg/mL on a sizing column as well (Figure 24). However, when the two are dialyzed in urea and subsequently dialyzed into a refolding buffer, a heterodimer forms and cleavage products become present as shown in the chromatogram in figure 25. There are five peaks that were resolved on the column and correspond to 73 kDa, 37 kDa, 27 kDa, 11 kDa, and 6 kDa. Procaspase-8 has a molecular weight of 29.5 kDa and the full length FLIP has a molecular weight of 37 kDa. FLIP contains a large subunit of 27 kDa and a small subunit of 10 kDa. The largest peak represents 27 kDa and is therefore the elution of procaspase-8 and possibly the FLIP large subunit. This peak is slightly overlaid with the 36 kDa peak which represents the full length FLIP monomer. The 73 kDa peak corresponds to the caspase-8-FLIP heterodimer or a possible FLIP homodimer. The 11 kDa peaks corresponds to the small subunit of FLIP.

REFERENCES

1. Pop, C., G.S. Salvesen, and F.L. Scott, *Chapter 21 Caspase Assays: Identifying Caspase Activity and Substrates In Vitro and In Vivo.* 2008. **446**: p. 351-367.
2. Pop, C., et al., *FLIP(L) induces caspase 8 activity in the absence of interdomain caspase 8 cleavage and alters substrate specificity.* Biochem J, 2011. **433**(3): p. 447-57.
3. Chen, Y.R. and A.C. Clark, *Kinetic traps in the folding/unfolding of procaspase-1 CARD domain.* Protein Sci, 2004. **13**(8): p. 2196-206.
4. Bolen, M.S.a.D.W., *Unfolding free energy changes determined by the linear extrapolation method. 1. Unfolding of phenylmethanesulfonyl alpha-chymotrypsin using different denaturants.* American Chemical Society, 1988. **442**: p. 123-132.
5. Walters, J., et al., *Allosteric modulation of caspase 3 through mutagenesis.* Biosci Rep, 2012. **32**(4): p. 401-11.
6. Walters, J., S.L. Milam, and A.C. Clark, *Chapter 1 Practical Approaches to Protein Folding and Assembly.* 2009. **455**: p. 1-39.
7. Mackenzie, S.H. and A.C. Clark, *Slow folding and assembly of a procaspase-3 interface variant.* Biochemistry, 2013. **52**(20): p. 3415-27.
8. Boatright, K.M., et al., *A unified model for apical caspase activation.* Mol Cell, 2003. **11**(2): p. 529-41.
9. Kelly M. BOATRIGHT, C.D., Jean-Bernard DENAULT, Daniel P. SUTHERLIN and Guy S. SALVESEN, *Activation of caspases-8 and -10 by $FLIP_{(L)}$.* Biochemistry, 2004. **382**: p. 651-657.

10. Pop, C., et al., *Role of proteolysis in caspase-8 activation and stabilization.* Biochemistry, 2007. **46**(14): p. 4398-407.

11. Yu, J.W., P.D. Jeffrey, and Y. Shi, *Mechanism of procaspase-8 activation by c-FLIPL.* Proc Natl Acad Sci U S A, 2009. **106**(20): p. 8169-74.

FIGURES

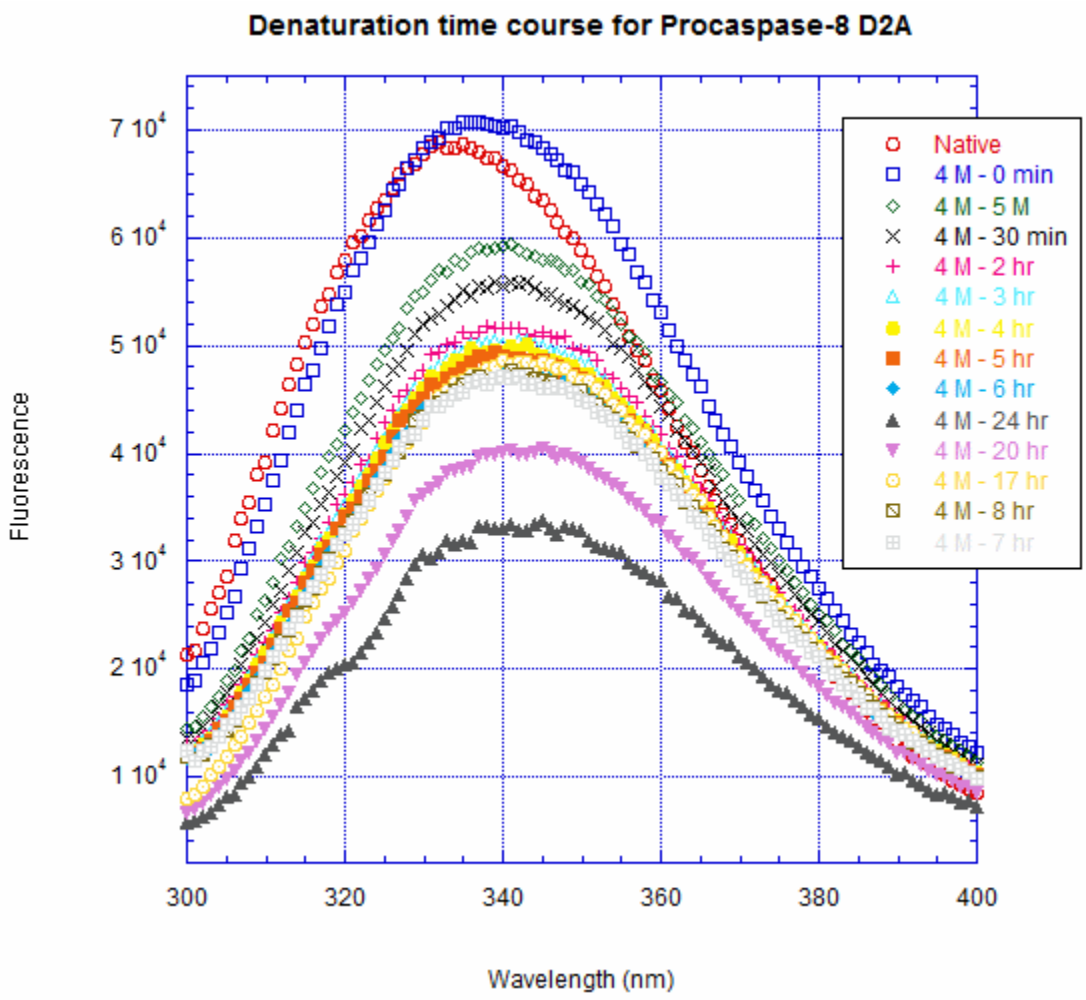

Figure 1: Fluorescence emission spectra of 1 uM procaspase-8. Excitation at 280 nm. Procaspase-8 was incubated up to 24 hours in 4 M urea.

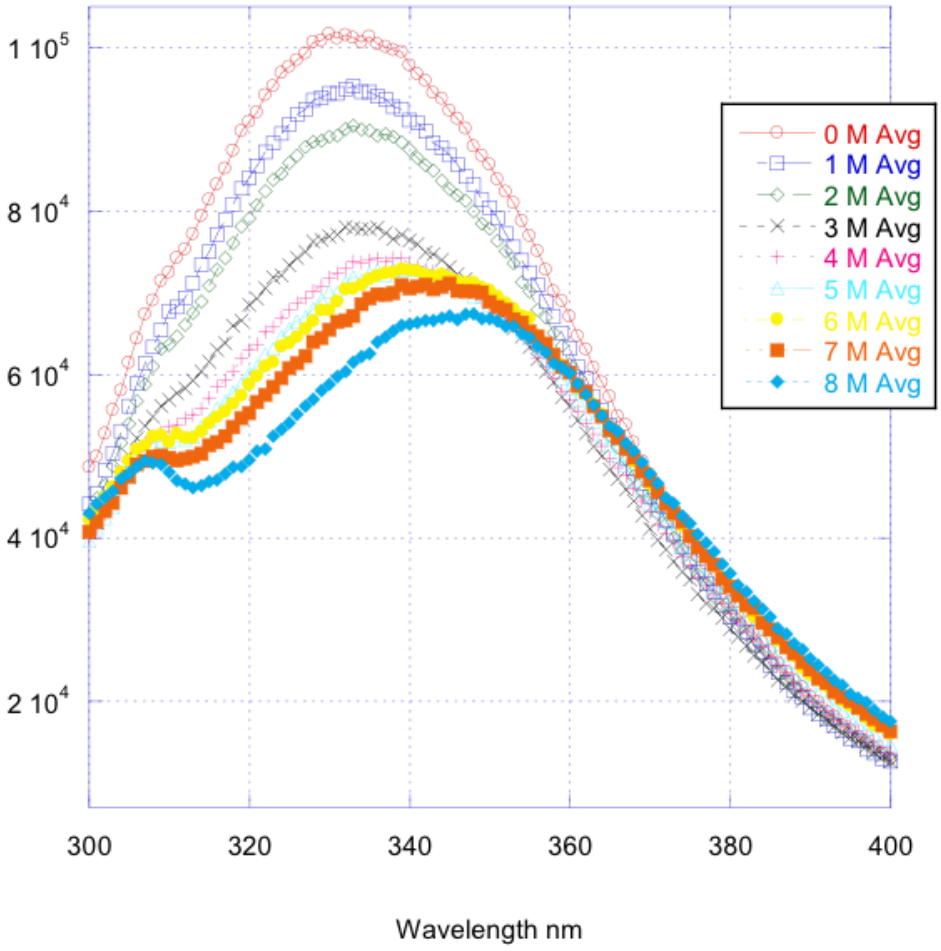

Figure 2: Fluorescence emission spectra of 1 uM procaspase-8 in 0 – 8 M urea at 1 M increments. Average taken of three repeats on different purifications. Error bars omitted for clarity. Excitation 280 nm.

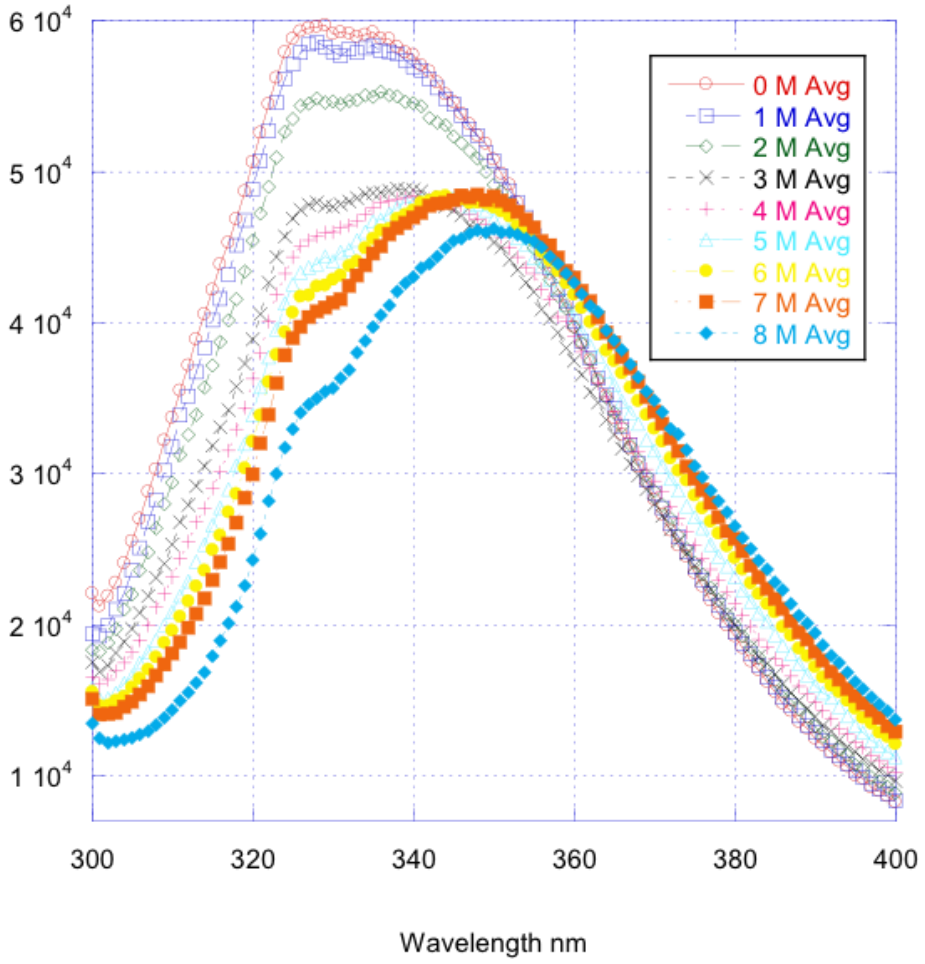

Figure 3: Fluorescence emission spectra of 1 uM procaspase-8 in 0 – 8 M urea at 1 M increments. Average taken of three repeats on different purifications. Error bars omitted for clarity. Excitation 295 nm.

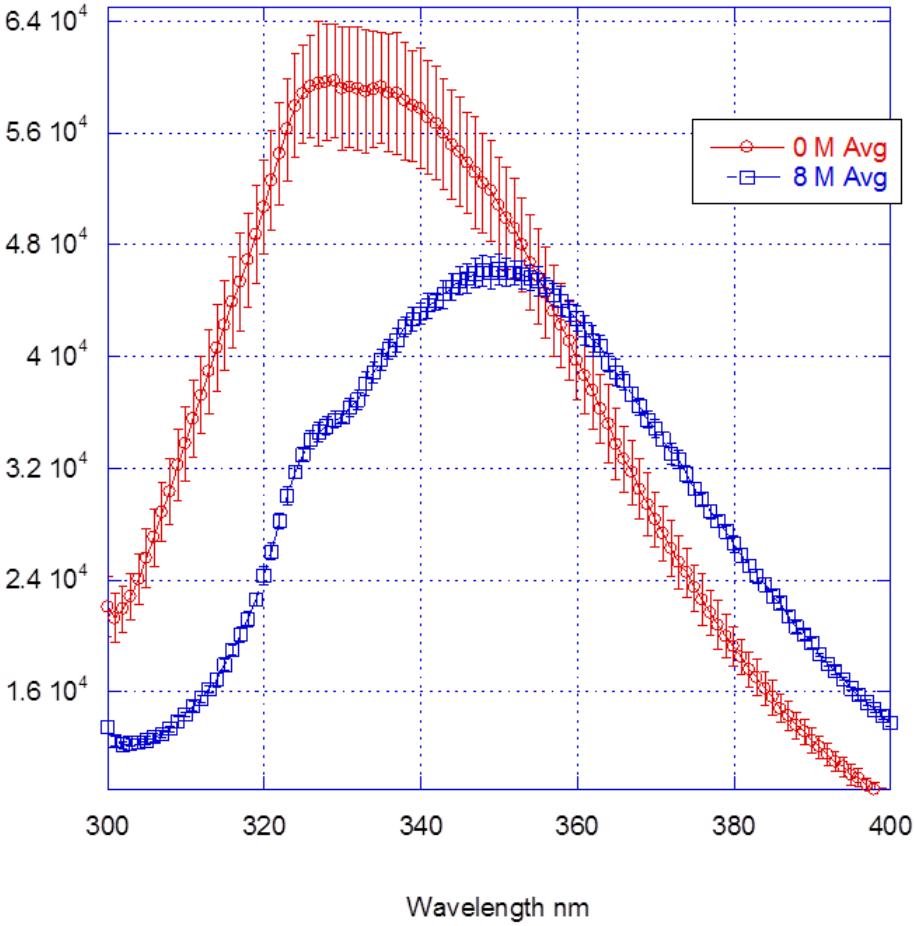

Figure 4: Fluorescence emission spectra of 1 uM procaspase-8 in 0 and 8 M urea. Average taken of three repeats on different purifications. Error taken as a standard deviation, Excitation 295 nm.

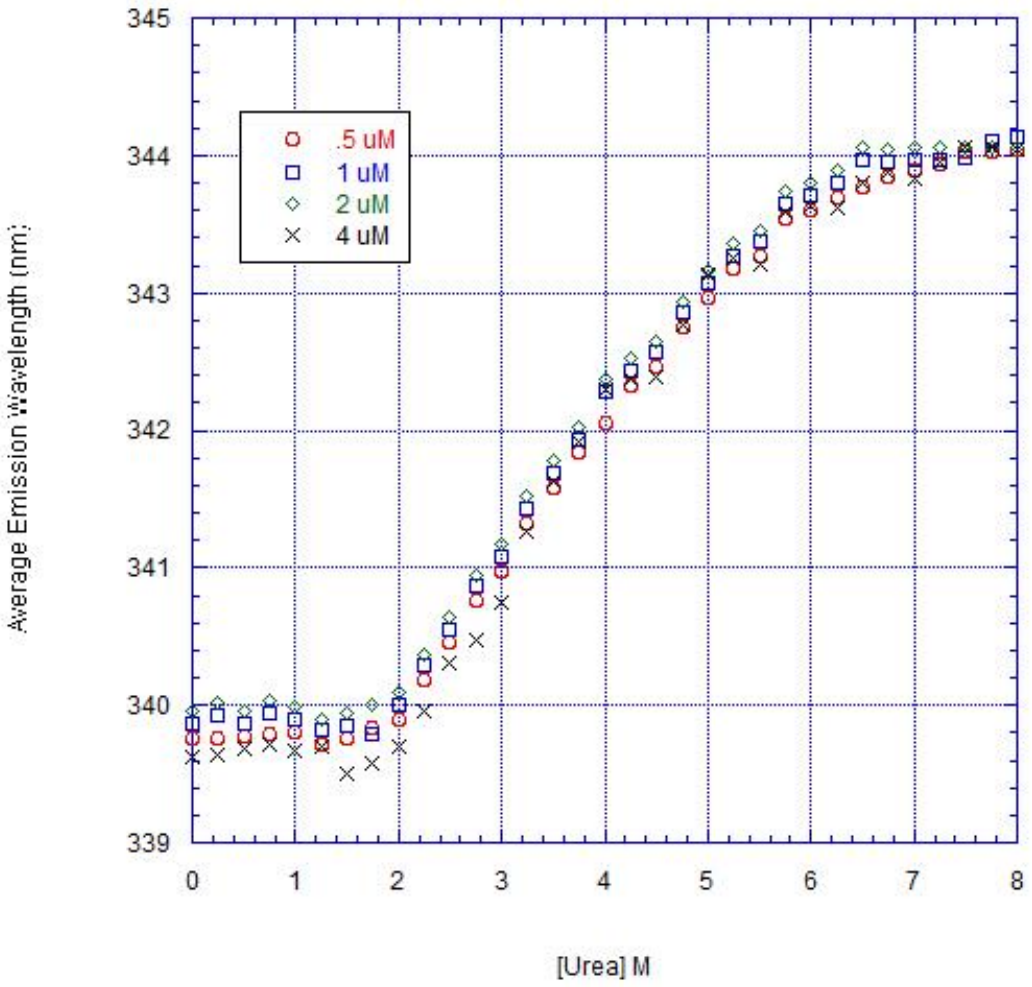

Figure 5: Average emission wavelength spectra of 0.5, 1, 2, and 4 uM procaspase-8 in 0 – 8 M urea. Average taken of three repeats on different purifications. Excitation 280 nm.

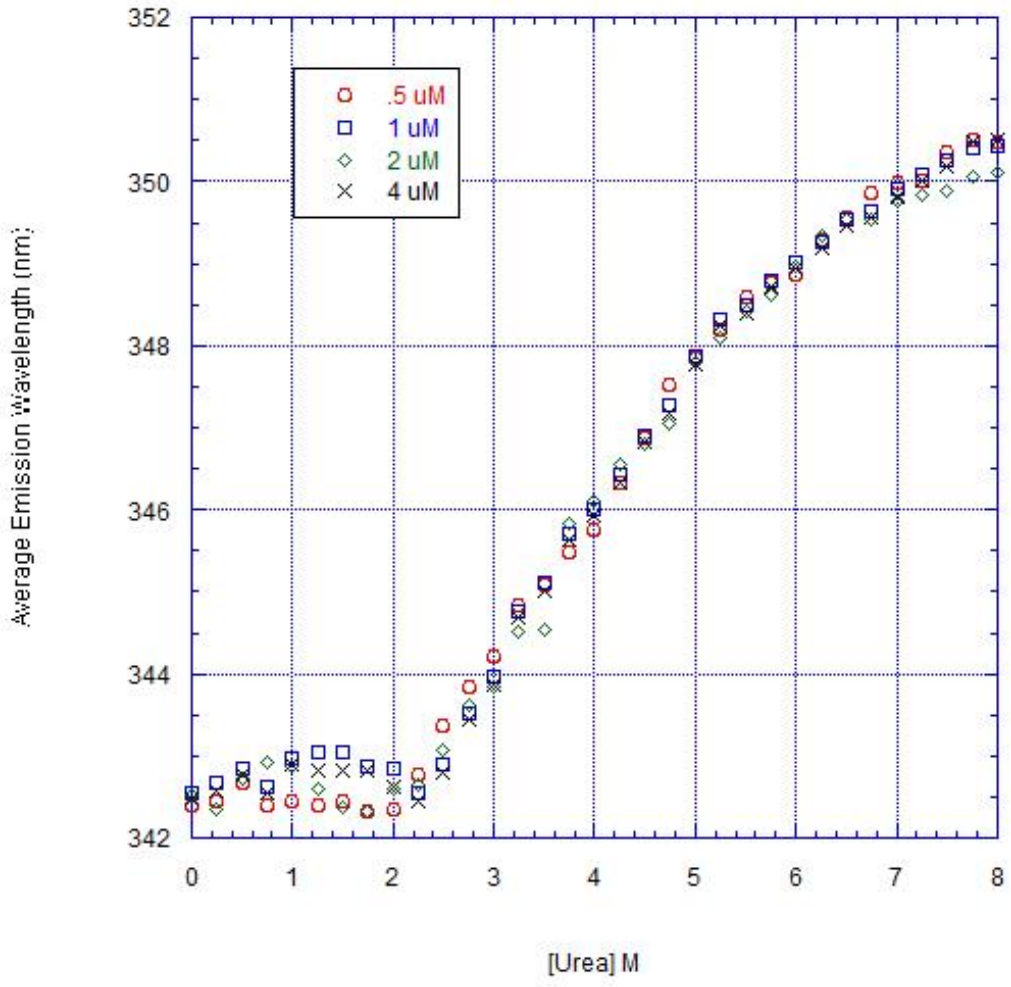

Figure 6: Average emission wavelength spectra of 0.5, 1, 2, and 4 uM procaspase-8 in 0 – 8 M urea. Average taken of three repeats on different purifications. Excitation 295 nm.

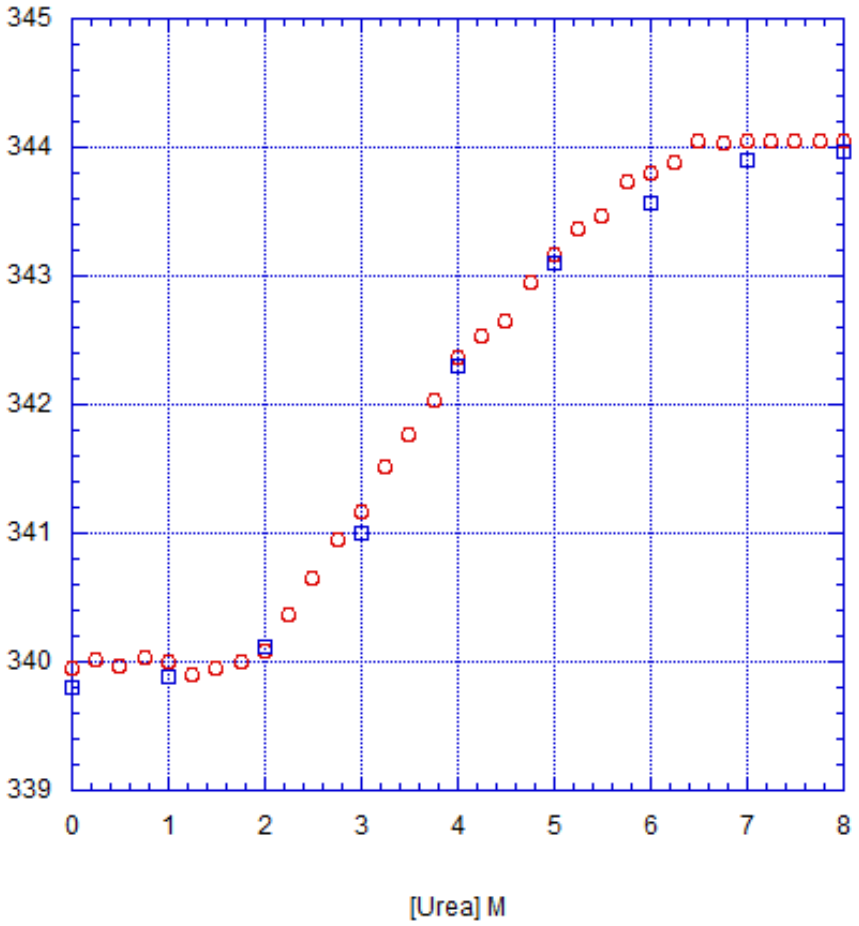

Figure 7: Average emission wavelength in nm. Reversibility of figure 7 was determined by unfolding procaspase-8 and then dialyzing out the urea to whole number increments from 8 to 1 M urea. Excitation 280 nm. 2 uM procaspase-8 shown in red and 2 uM refolding shown in blue.

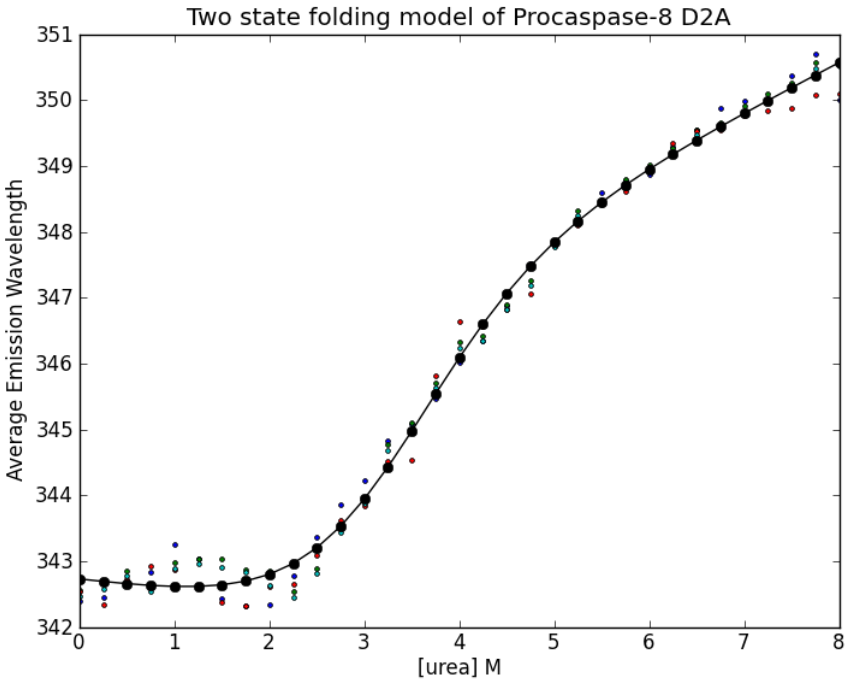

Figure 8: Two-state fit model for the average emission wavelength data of procaspase-8.

Table 1: Thermodynamic parameters for zC8 determined by the two-state folding model and non-linear least squares regression fitting routine in python.

Table 1

$Y_f = 342.628\, nm$
$m_f = .432$
$Y_u = 353.25\, nm$
$m_u = -0.3507$
$m = -1.067 \frac{kCal}{mol}/M$
$\Delta G = 4.4711\ kCal/mol$

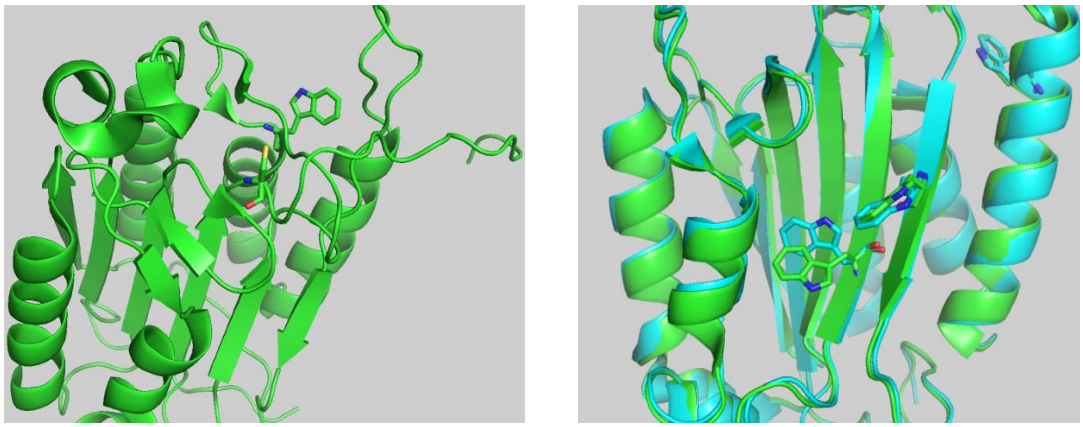

Figure 9: (A) Procaspase-8 shown as a cartoon with the catalytic cysteine and tryptophan residue shown as stick models. PDB: 3H12 (B) $FLIP_{(L)}$ shown as a cartoon with the tryptophan residues highlighted as stick models. Cyan corresponds to the monomeric form of the protein and green corresponds to the heterodimeric form. PDB: 3H13 (monomer) and 3H11 (heterodimer).

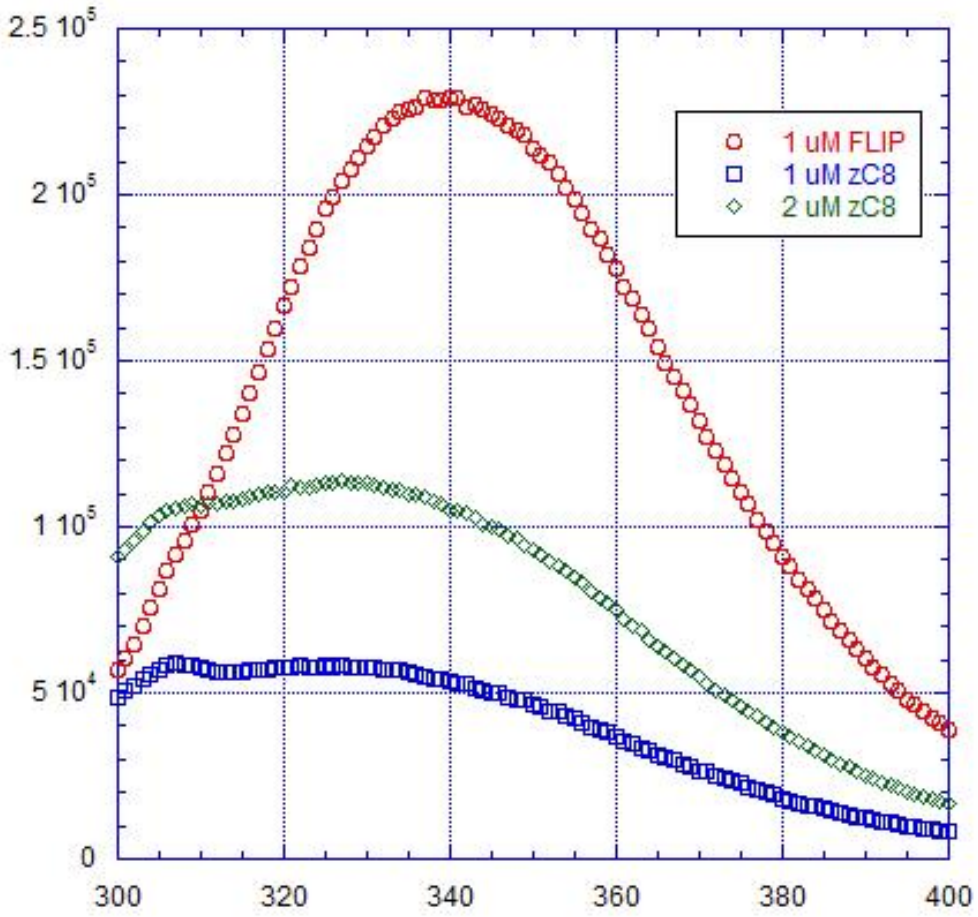

Figure 10: Comparison of the raw fluorescence data of procaspase-8 at 1 and 2 uM and FLIP at 1 uM. Excitation at 280 nm.

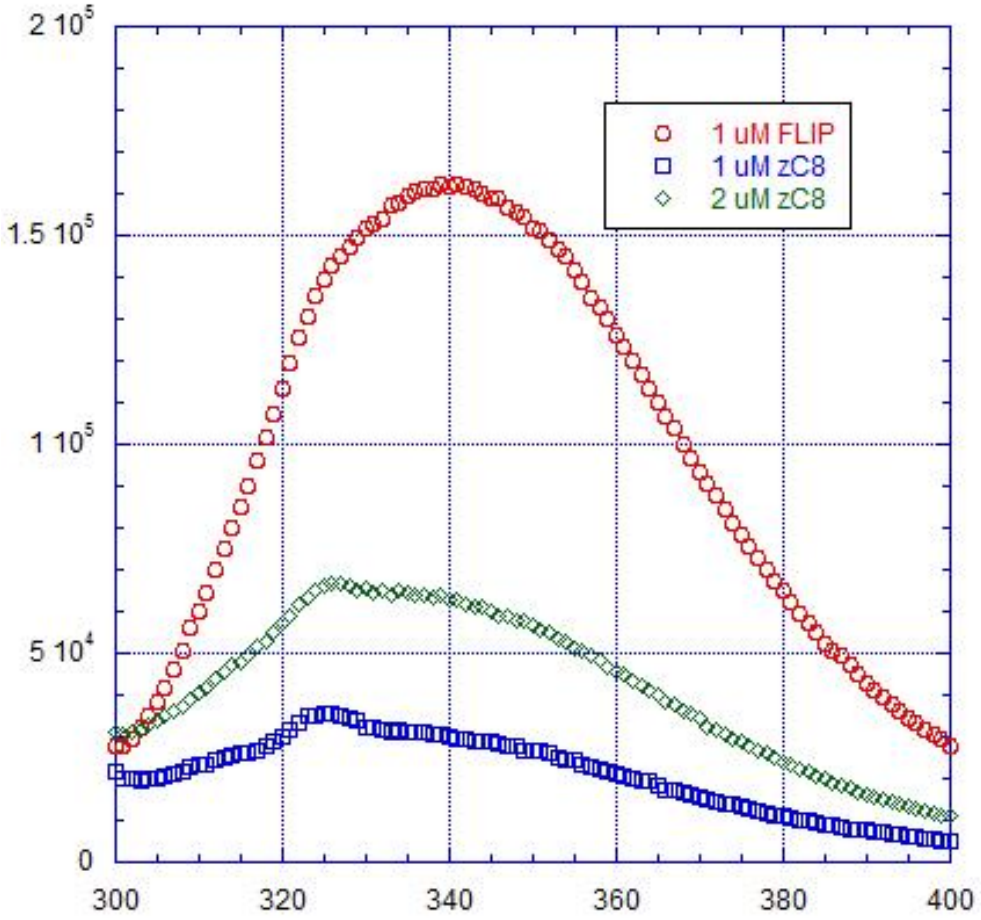

Figure 11: Comparison of the raw fluorescence data of procaspase-8 at 1 and 2 uM and FLIP at 1 uM. Excitation at 295 nm.

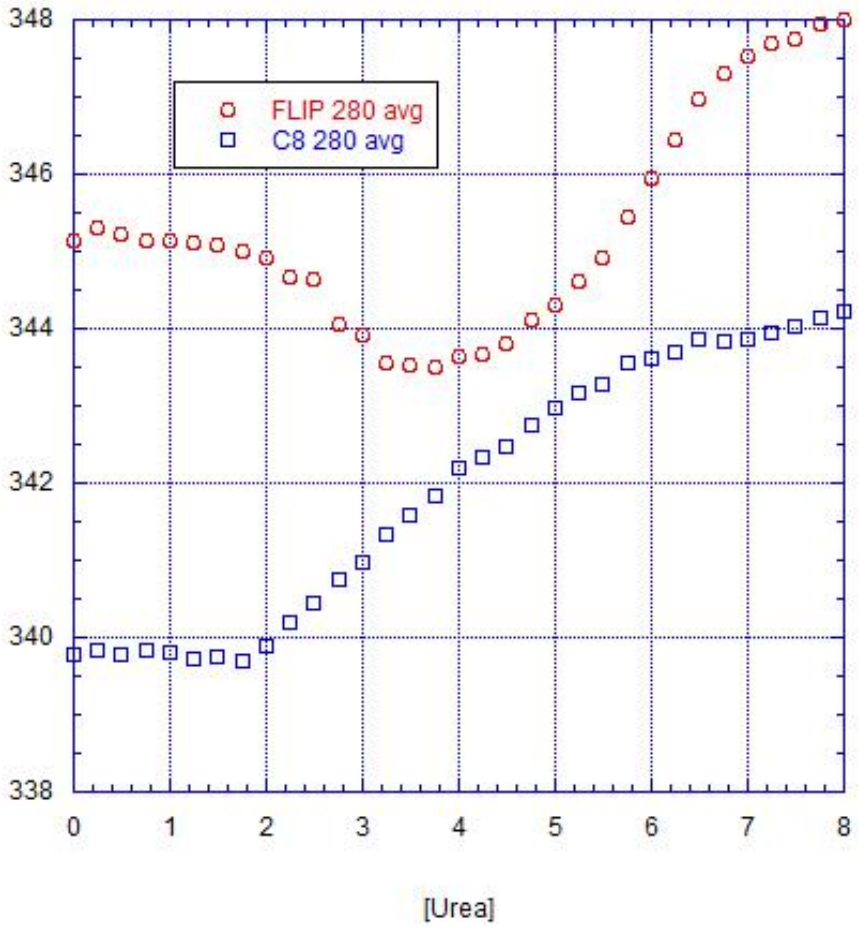

Figure 12: Comparison of the average emission wavelength change upon denaturation of procaspase-8 (blue) and FLIP (red). Excitation 280 nm.

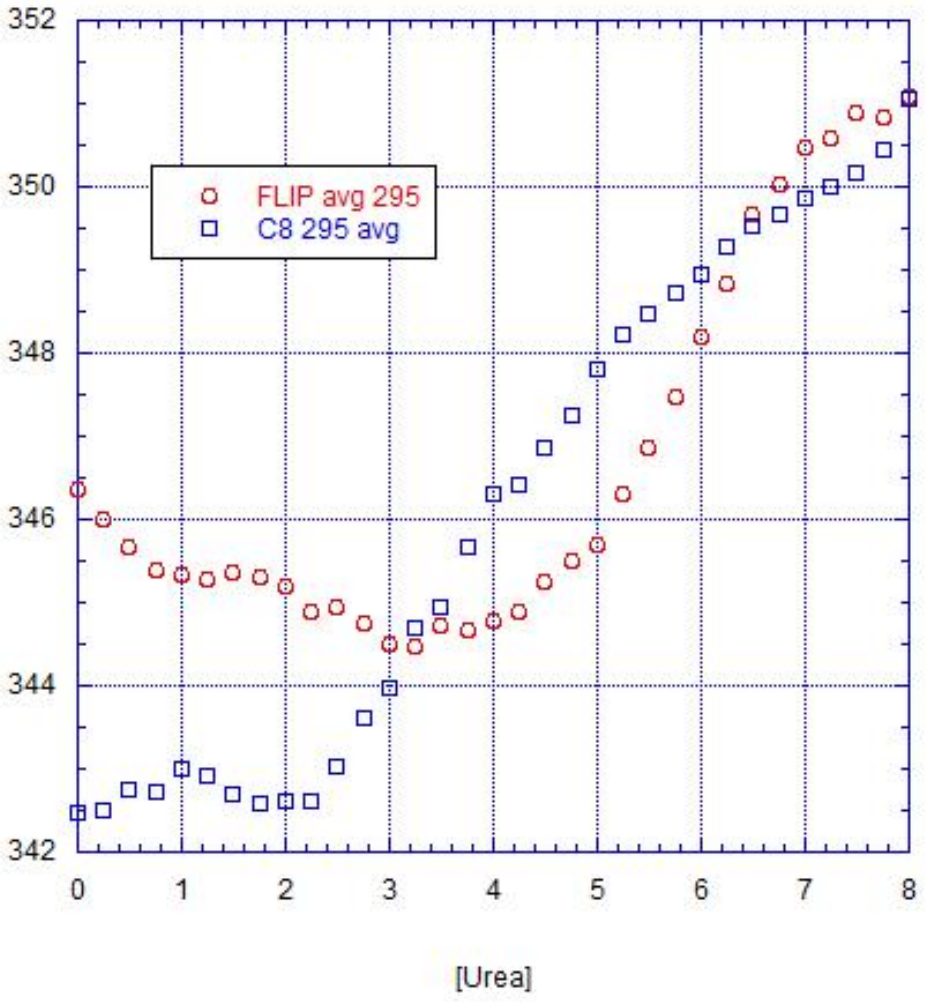

Figure 13: Comparison of the average emission wavelength change upon denaturation of procaspase-8 (blue) and FLIP (red). Excitation 295 nm.

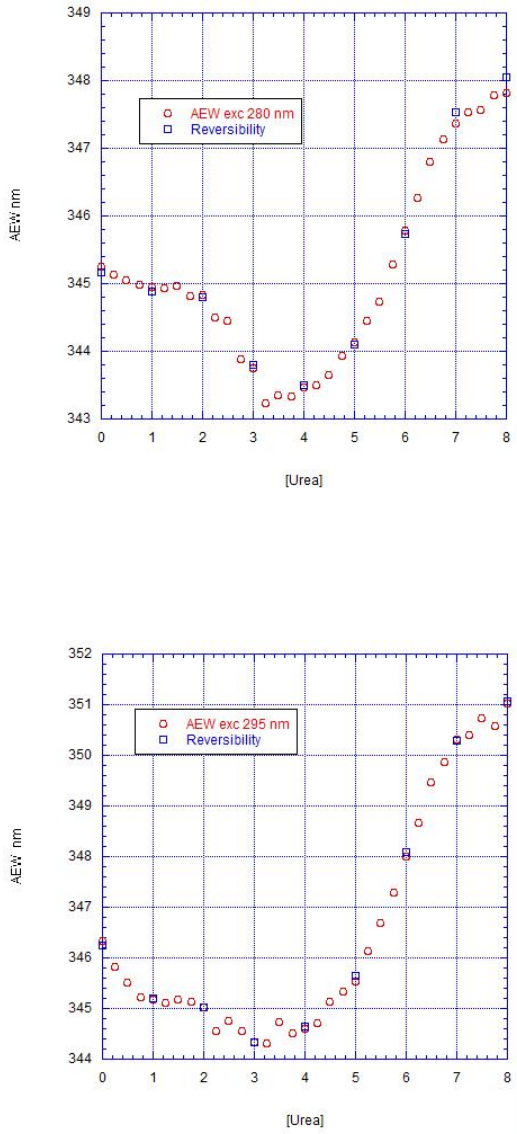

Figure 14: Reversibility of the unfolding pathway of FLIP. Top, excitation 280 nm and bottom, excitation at 295 nm.

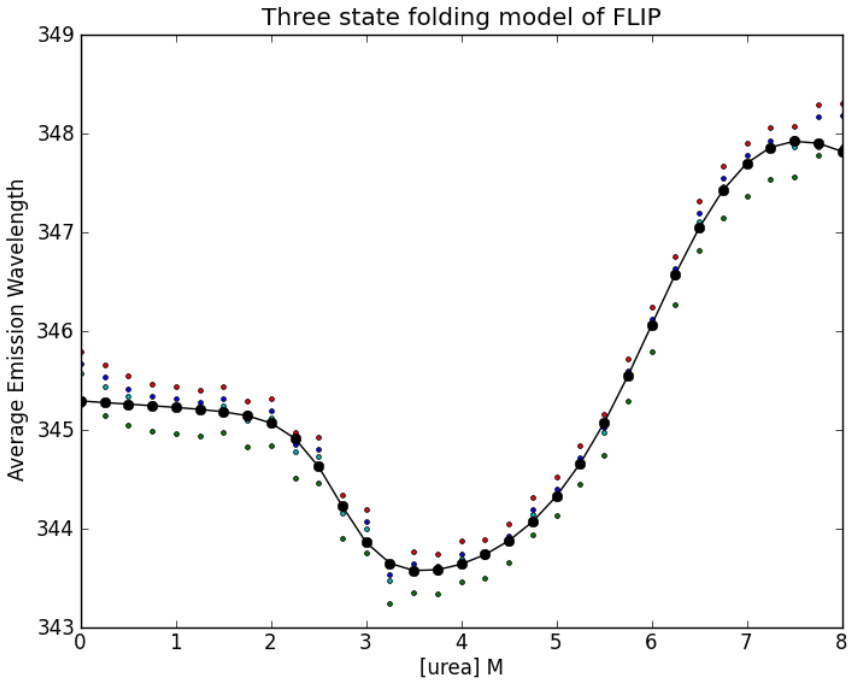

Figure 15: The three state folding model of FLIP. Red dots are 2 uM FLIP, blue dots represent 4 uM FLIP, turquoise dots are .5 uM FLIP, and the green dots represent 1 uM FLIP.

Table 2: Thermodynamic parameters determined by the two-state folding model for FLIP.

Table 2

$Y_f = 345.28\,nm$
$m_f = -.0632$
$Y_u = 342.7\,nm$
$m_u = -.2411$
$Y_i = 343.38\,nm$
$m_1 = -2.27\,\frac{kj}{mol}/M$
$m_1 = -.9089\,\frac{kj}{mol}/M$

$\Delta G_1^{HOH} = 6.209\ kJ/mol$
$\Delta G_2^{HOH} = 5.657\ kJ/mol$

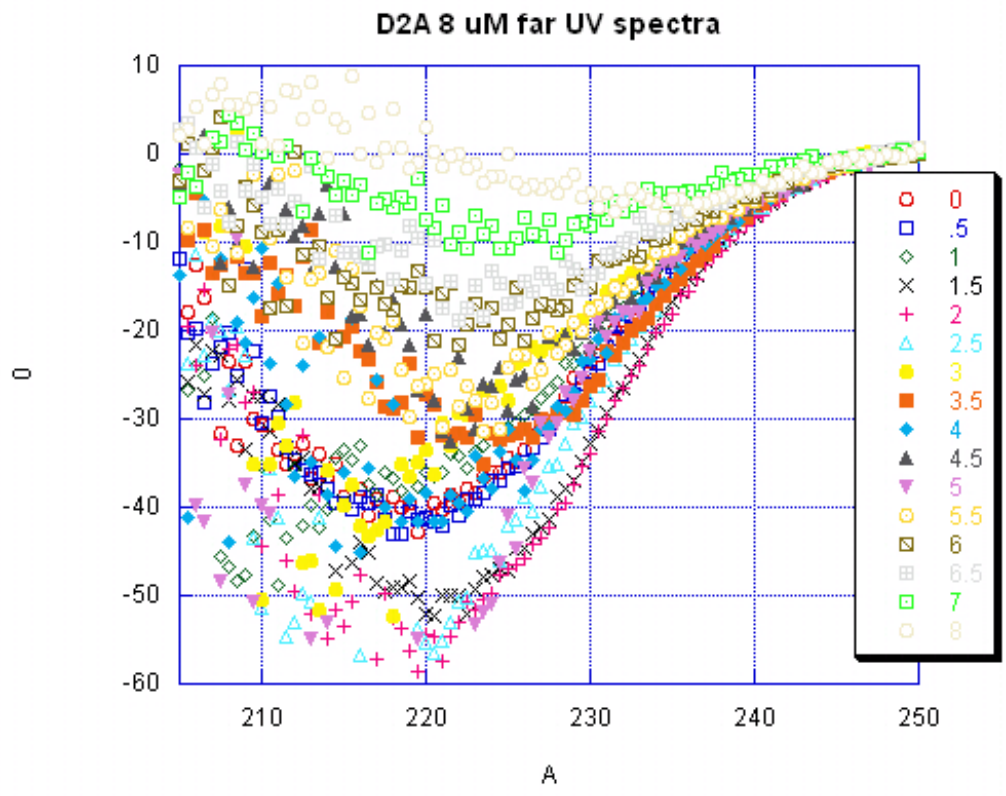

Figure 16: Far UV spectra of procaspase-8 in 0 to 8 M urea of procaspase-8.

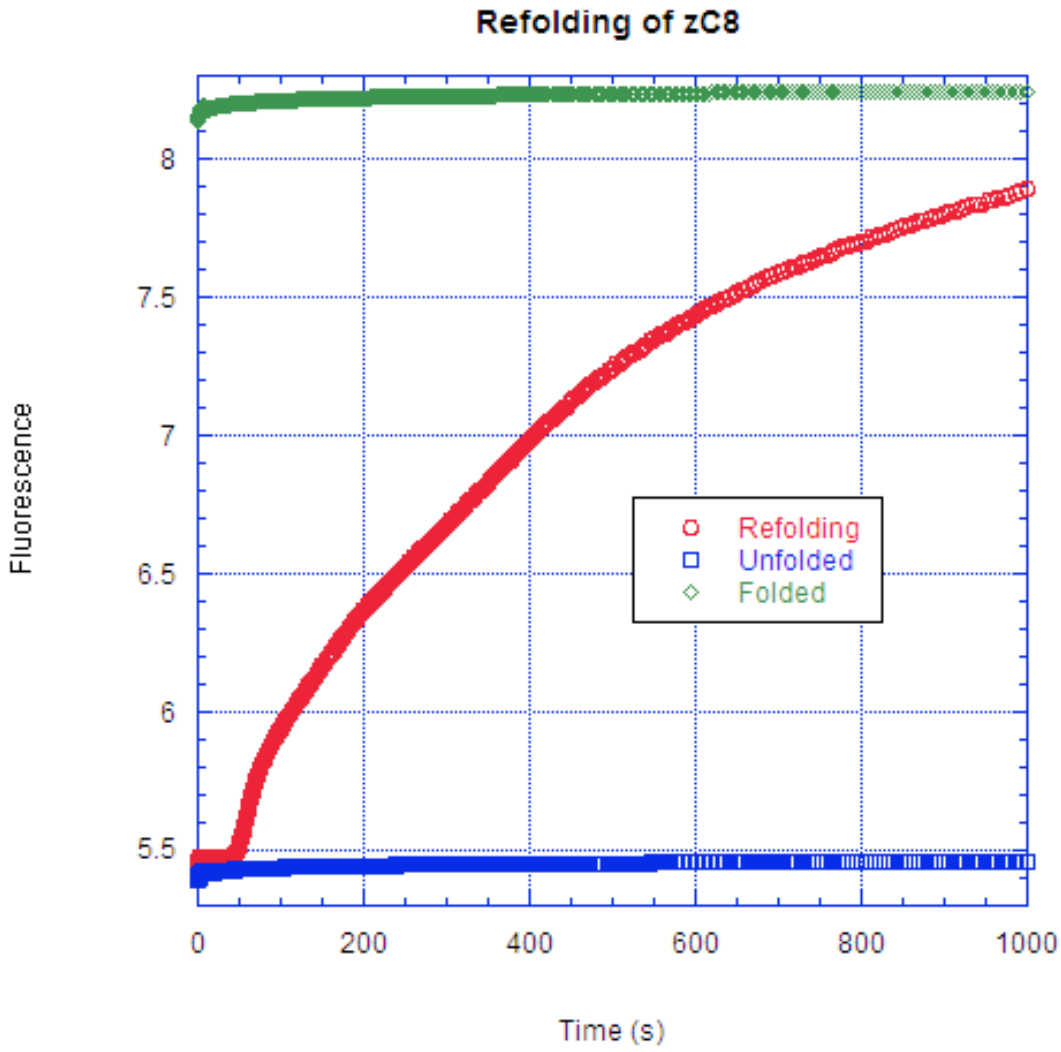

Figure 17: Kinetic refolding of procaspase-8. The folded species is shown in green and the unfolded species is shown in blue. The refolding process is shown to contain a lag phase for 60 seconds followed by an exponential growth phase shown in red. Excitation 280 nm.

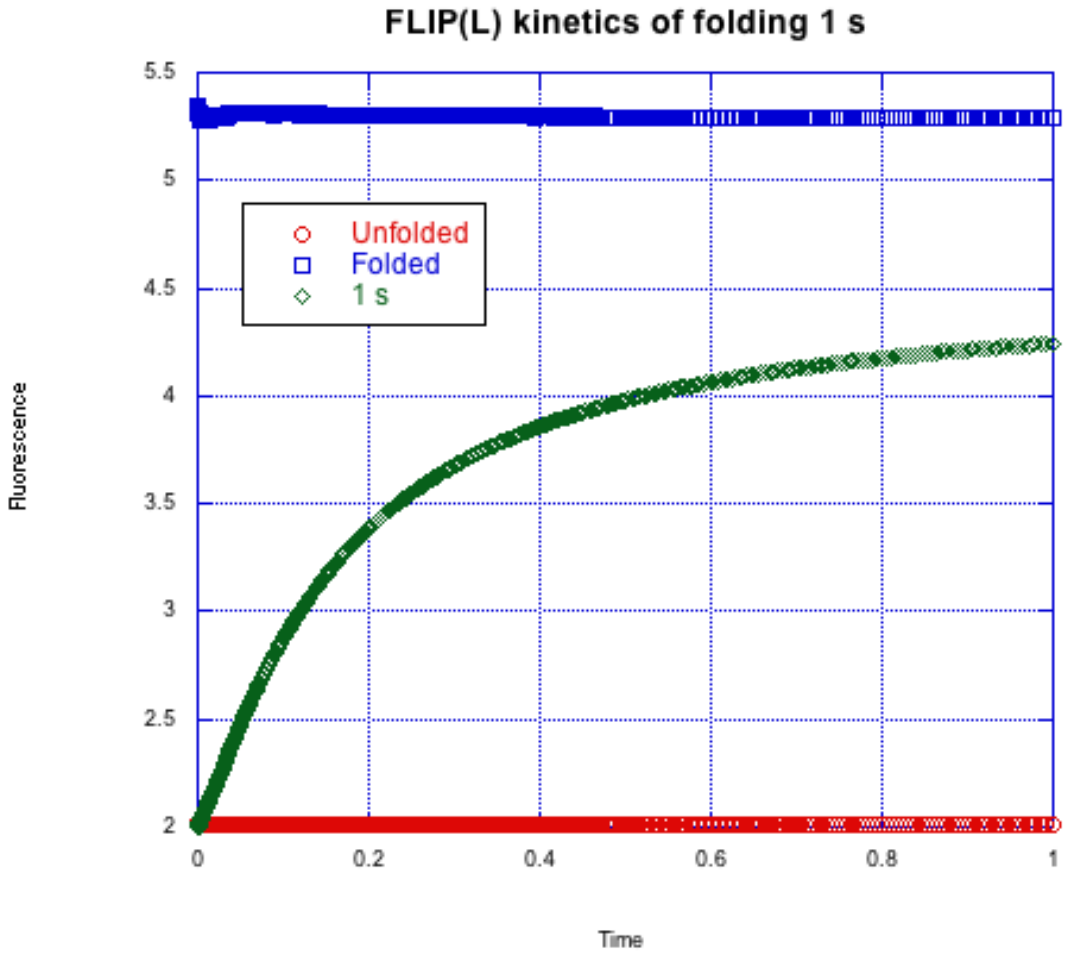

Figure 18: Kinetic refolding of FLIP. The folded species is shown in blue and the unfolded species is shown in red. The refolding process is shown to contain an exponential growth phase shown in green. Excitation 280 nm.

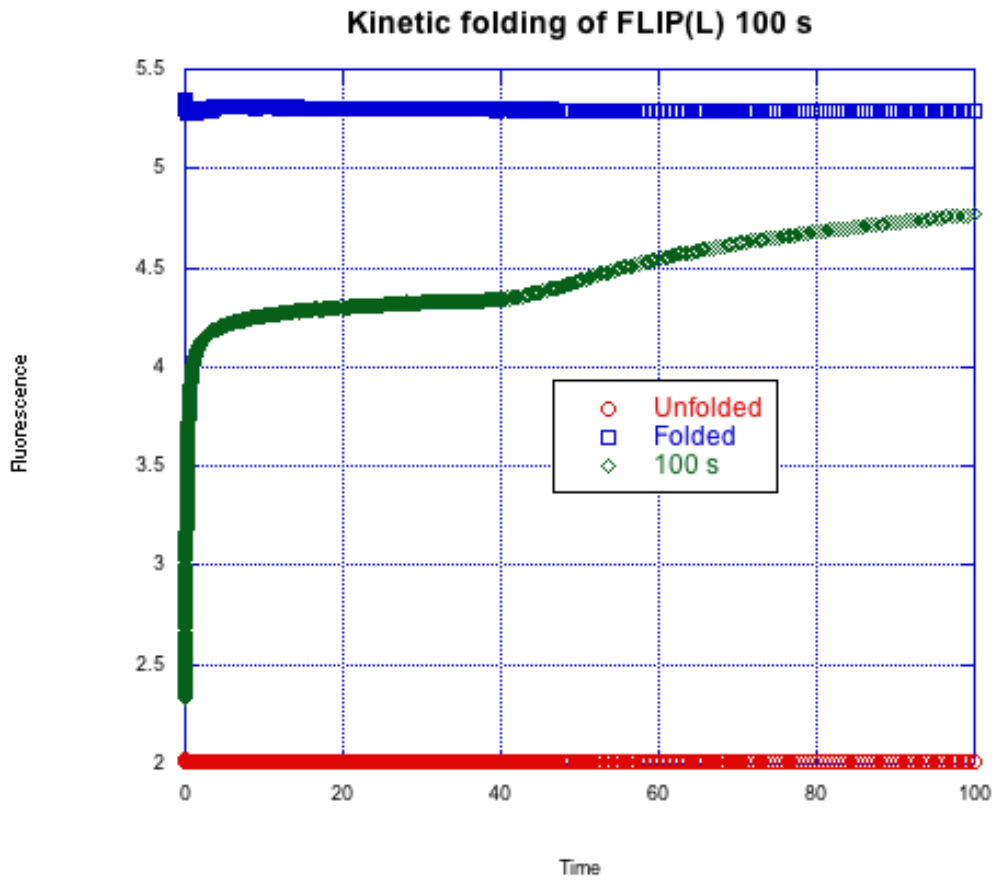

Figure 19: Kinetic refolding of FLIP. The folded species is shown in blue and the unfolded species is shown in red. The refolding process is shown to contain an exponential growth phase followed by a second exponential phase shown in green. Excitation 280 nm.

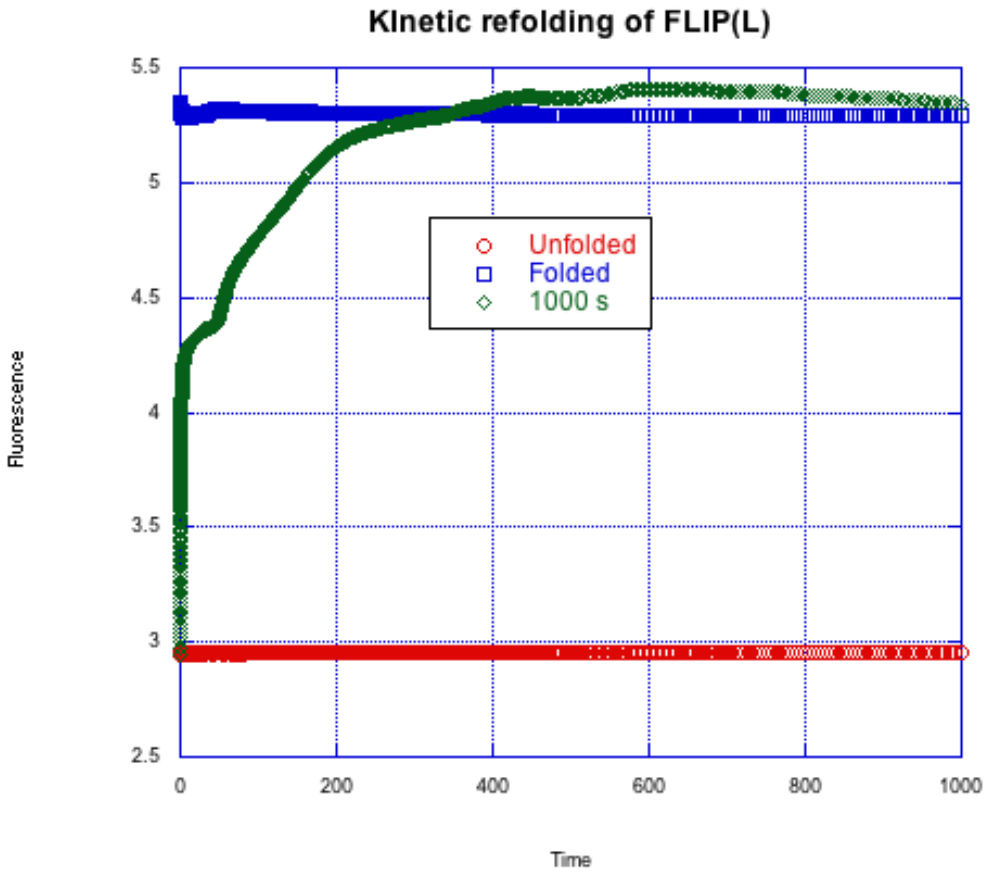

Figure 20: Kinetic refolding of FLIP. The folded species is shown in blue and the unfolded species is shown in red. The refolding process is shown to contain an exponential growth phase followed by a second exponential phase shown in green and a return to the native state. Excitation 280 nm.

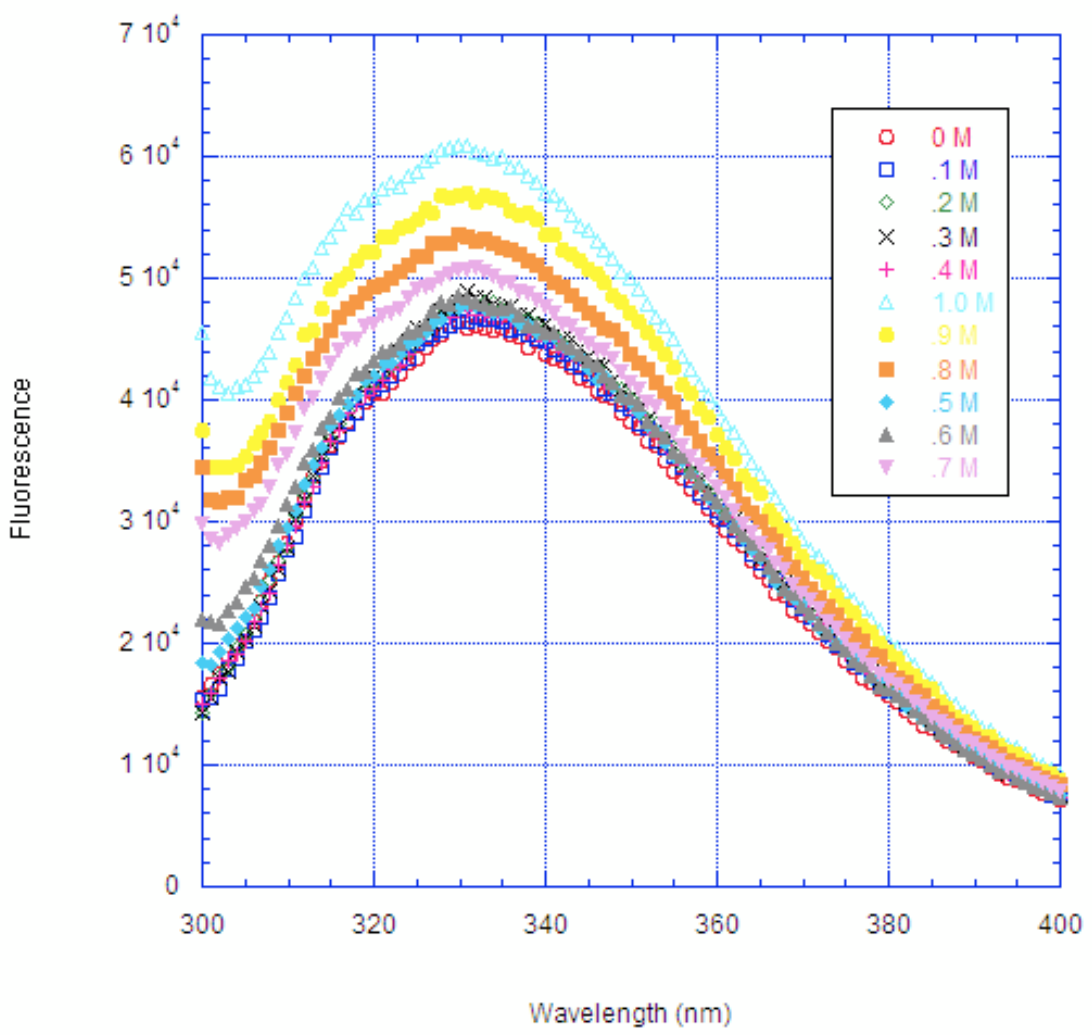

Figure 21: Raw fluorescence data of 2 uM procaspase-8 dimerization in increasing concentrations of sodium citrate from 0 to 1 M in 0.1 M increments. Excitation 280 nm.

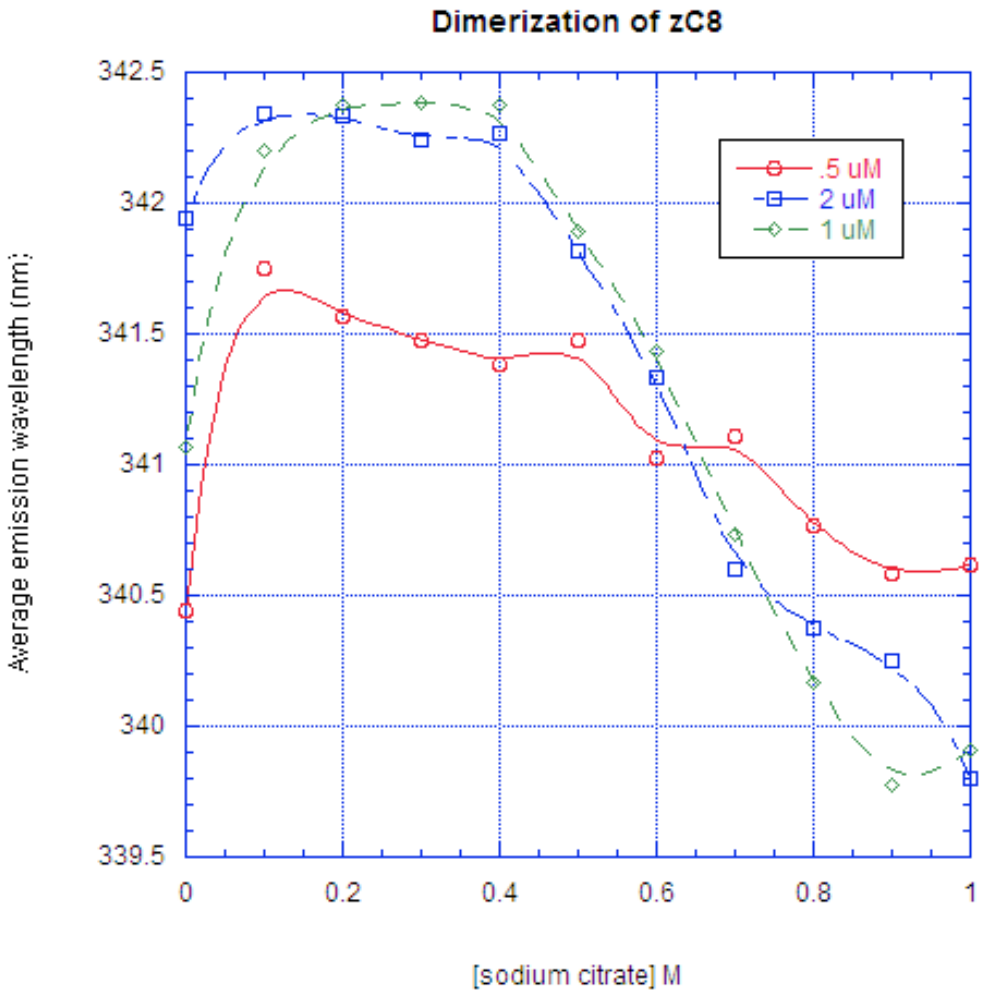

Figure 22: Average emission wavelength profile of caspase-8 dimerization in sodium citrate. Sodium citrate ranges from 0 to 1 M in 0.1 M increments. 0.5, 1, and 2 uM procaspase-8 were used to determine concentration dependent changes in signal.

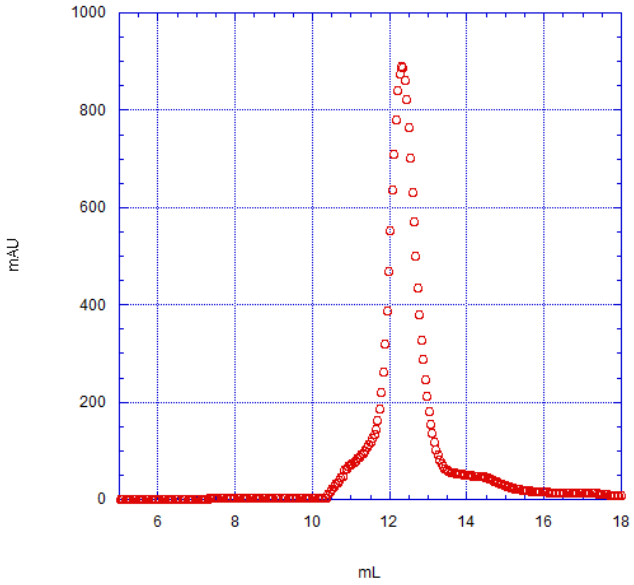

Figure 23: 1 mg/mL DED-less procaspase-8 D2A elution profile on a sizing column. The elution volume is 12.31 mL corresponding to a molecular weight of 26.5 kDa.

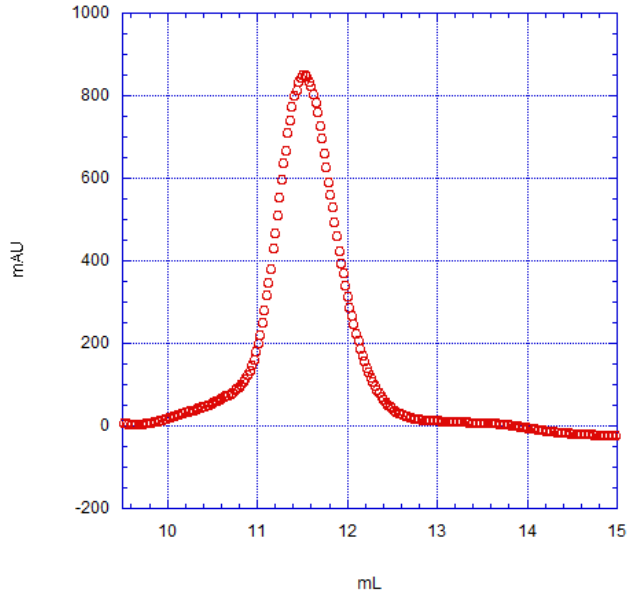

Figure 24: 1 mg/mL DED-less FLIP elution profile on a sizing column. The elution volume is 11.51 mL corresponding to a molecular weight of 36 kDa.

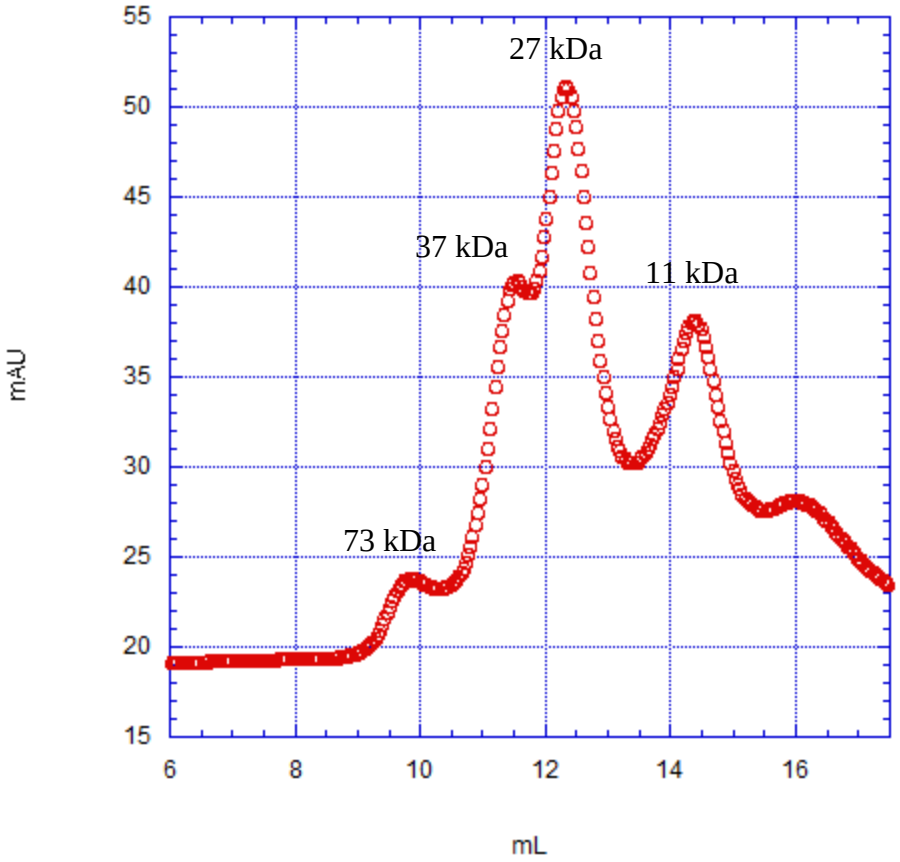

Figure 25: Chromatogram of procaspase-8 and FLIP after urea-induced unfolding (4 M) and subsequent dialysis into a refolding buffer.

CHAPTER IV

Discussion

Protein folding studies elucidate the function of proteins. Furthermore, understanding how proteins fold from their primary structure of amino acids into a functional quaternary structure is important in understanding how proteins interact with other proteins, catalyze reactions, and perform various functions for cells. Determining a folding mechanism of a holoenzyme and the individual domains that comprise the holoenzyme can yield valuable information toward understanding the stability and formation of the holoenzyme itself. Procaspase-8 presents an interesting folding problem that we examined: do homologous proteins fold along the same path and among the homologous proteins that heterodimerize, what conditions favor heterodimerization? It has been shown previously that uncleavable procaspase-8 exists predominantly in its monomeric form (>97%) at equilibrium and wild type procaspase-8 exists in a slow equilibrium with the dimeric form [1]. Furthermore, uncleavable procaspase-8 can only manage <1% activity. Upon heterodimerization with the homologous protein FLIP, uncleavable procaspase-8 is activated to near wild-type activity [2]. To date, very few laboratories have examined the biophysical properties of procaspase-8 and none have elucidated the procaspase-8 or FLIP folding mechanism. Our study is a biophysical comparison of the procaspase-8 and FLIP monomers and the formation of the caspase-8 dimer and caspase-8-FLIP heterodimer. We have examined the equilibrium unfolding and kinetic folding of procaspase-8 and FLIP to determine the mechanism and rate of folding in order to understand how the homodimer and heterodimer form.

The equilibrium experiments show that monomeric procaspase-8 and FLIP fold very differently. Procaspase-8 folds via a two-state model and has a urea1/2 of 4 M. In contrast, FLIP folds via a three-state model with an intermediate at 4M urea and a urea1/2 of 6 M.

This adds more evidence to the relatively accepted theory that homologous proteins do not fold along the same path because they differ in their primary structure. Both proteins exhibit reversibility in their folding pathway and show no concentration dependencies. FLIP's aromatic content in generally more solvent exposed and thus has an average emission wavelength higher than that of procaspase-8. FLIP contains an intermediate in its folding pathway where the tryptophan residues are more buried than in the native state of the protein. The convenient location of a single tryptophan in the active site of procaspase-8 also allows us to correlate intrinsic fluorescence emission with active site changes upon urea denaturation and also kosmotrope dimerization. The dimerization of procaspase-8 results in the initial shift of the active site tryptophan residue into a hydrophobic environment and then to a more solvent exposed one upon dimerization. This confirms what is seen in crystal structures as the tryptophan is in line with the S2 and S4 sub site and it also hydrogen bonds with the Ac-IETD-cho inhibitor in a solvent exposed position [3]. We conclude that dramatic changes occur in the solvent accessibility of the tryptophan residue during dimerization corresponding to the large active site changes that occur upon dimerization and activation of caspase-8 reported by others. FLIP has 2 tryptophan residues in its dimer interface and the intrinsic fluorescence measurements can give us some clues as to when the dimer interface is more or less solvent exposed. A major pitfall to this logic is the presence of a third tryptophan in a relatively solvent exposed position on the other side of the monomer. In 4 M urea, the tryptophan residues of FLIP are in their most buried position which could correspond to a more hydrophobic dimer interface environment.

The kinetic folding experiments yielded important results for both the folding of procaspase-8 and FLIP monomers. Stopped-flow fluorescence spectroscopy was used to determine the folding kinetics of procaspase-8 and FLIP. 22 uM unfolded procaspase-8 was rapidly diluted from 8 M urea to 0.72 M urea to initiate folding. Procaspase-8 folds slowly and remains in a lag phase for the first 60 seconds of folding. While we were not able to resolve the signal equilibrate to the folded signal, we can extrapolate that the entire folding process takes approximately 1300 seconds. The reason for the slower folding could be that the secondary structural elements are not stable. It has also been shown through a bioinformatics study that proteins with long range contacts involved in the folding of the protein core and the hydrophobicity of that core influences the folding rate. Even though FLIP is homologous to procaspase-8 it folds nearly 1000 seconds faster. FLIP reaches the folded signal after approximately 300 seconds of folding. Within the first second of folding, FLIP has reached over 50% of the native structure's signal. The kinetic folding profile of FLIP also shows possible ultrastructured species which lie above the folded signal. This could correspond to a possible FLIP-homodimer or simply aggregation.

Size exclusion chromatography experiments were performed to determine the oligomeric status of procaspase-8 and FLIP and also determine if FLIP was cleaved. We hypothesized that procaspase-8 and FLIP would heterodimerize upon population of the intermediate state in the folding pathway of FLIP and population of the urea1/2 for procaspase-8 in 4 M urea and subsequent dialysis into a refolding buffer. Upon heterodimerization, FLIP would become cleaved to its large and small subunit but would stay intact with procaspase-8. There is growing research that once FLIP is cleaved, the small

subunit detaches from the holoenzyme leaving a p42 active enzyme [4]. The full length heterodimer is 67 kDa in size. However, the chromatogram shows a peak corresponding to 73 kDa which could represent a FLIP dimer. The kinetics data also show a possible dimer as an ultrastructured species moves beyond the folded signal of FLIP. The existence of a FLIP homodimer has never been published. The 73 kDa peak could also correspond to the caspase-8-FLIP heterodimer in its 67 kDa form. In this case it is likely that the heterodimer does not fit with the hydrodynamic volumes of the standards and thus its size is not able to be accurately predicted. The next peak corresponds to 36 kDa representing the full length FLIP monomer. However, this large peak has a large width associated with it and could possibly contain a small p42 peak which cannot be ruled out. FLIP was run through the column before the experiment to yield a single large peak of similar width. The third peak in the chromatogram corresponds to 26 kDa and most likely represents the small subunit of FLIP which is 26 kDa and also the full length procaspase-8 monomer. FLIP is present in a 2 to 1 ratio of procaspase-8 to encourage heterodimerization as described in [2]. The fourth peak corresponds to the FLIP small subunit at 11 kDa. In order for cleavage of FLIP to occur in the quantities we observe, a heterodimer must be present and leads us to conclude that the formation of the heterodimer is relatively short-lived and dissociates into its respective constituents upon cleavage that is, the large and small subunit of FLIP and also the procaspase-8 monomer. It can also be concluded that FLIP forms heterodimers and becomes cleaved more efficiently after populating its intermediate state before or during heterodimerization.

These results have great significance to the biology of procaspase-8 and FLIP in a survival and apoptotic function. The cleavage of FLIP in a heterodimeric structure with procaspase-8 leads to its dissociation as shown previously [5]. During NFκB activation, p42 caspase-8-FLIP heterodimers are able to cause much greater activation that the full length caspase-8-FLIP heterodimer [6]. Our work confirms the cleavage and presence of the large and small subunit of FLIP but is unable to accurately resolve the p42 complex. Upon cleavage of FLIP, it has also been shown that the heterodimer dissociates and leads to apoptosis of cell under conditions that quell the expression of FLIP [7]. In order to examine only heterodimer formation in the absence of FLIP cleavage, it will be necessary for future work to use an uncleavable FLIP variant.

The folding pathway of procaspase-8 is slow and could possibly depend on its prodomain to accelerate the folding pathway. Understanding how the prodomain of procaspase-8 folds with the catalytic domain is crucial in understanding the entire folding mechanism of procaspase-8. Future work will need to determine the folding of the prodomain alone and the full length procaspase-8 monomer to understand how the domains may stabilize each other. Our lab has published results on the dimer interface of procaspase-8 and optimizing dimer formation [8]. This paper falls short of obtaining *in vivo* results confirming an increase in apoptosis. Future work will need to determine if the mutants created for homodimerization are even more efficient at creating heterodimers with FLIP thereby actually inhibiting apoptosis.

REFERENCES

1. Mrudula Donepudi, A.M.S. and a.M.G.G. Christophe Briand, *Insights into the Regulatory Mechanism for Caspase-8 Activation.* Molecular Cell, 2003. **11**: p. 543-549.
2. Yu, J.W., P.D. Jeffrey, and Y. Shi, *Mechanism of procaspase-8 activation by c-FLIPL.* Proc Natl Acad Sci U S A, 2009. **106**(20): p. 8169-74.
3. Keller, N., et al., *Structural and biochemical studies on procaspase-8: new insights on initiator caspase activation.* Structure, 2009. **17**(3): p. 438-48.
4. Shirley, S. and O. Micheau, *Targeting c-FLIP in cancer.* Cancer Lett, 2013. **332**(2): p. 141-50.
5. Tschopp, O.M.a.J.r., *Induction of TNF Receptor I-Mediated Apoptosis Via Two Sequential Signaling Complexes.* Cell, 2003. **114**: p. 181-190.
6. Koenig, A., et al., *The c-FLIPL Cleavage Product p43FLIP Promotes Activation of Extracellular Signal-regulated Kinase (ERK), Nuclear Factor kappaB (NF-kappaB), and Caspase-8 and T Cell Survival.* J Biol Chem, 2014. **289**(2): p. 1183-91.
7. Micheau, O., et al., *The long form of FLIP is an activator of caspase-8 at the Fas death-inducing signaling complex.* J Biol Chem, 2002. **277**(47): p. 45162-71.
8. Ma, C., S.H. Mackenzie, and A.C. Clark, *Redesigning the procaspase-8 dimer interface for improved dimerization.* Protein Sci, 2014.